Published in final edited form as:
Coord Chem Rev. 2012 February 1; 256(3-4): 393–411. doi:10.1016/j.ccr.2011.10.011.

Mechanism of Nitric Oxide Synthase Regulation: Electron Transfer and Interdomain Interactions

Changjian Feng
Department of Pharmaceutical Sciences, University of New Mexico, Albuquerque, NM 87131 (USA) cfeng@unm.edu, Tel: 505-925-4326, Fax: 505-925-4549

Abstract

Nitric oxide synthase (NOS), a flavo-hemoprotein, tightly regulates nitric oxide (NO) synthesis and thereby its dual biological activities as a key signaling molecule for vasodilatation and neurotransmission at low concentrations, and also as a defensive cytotoxin at higher concentrations. Three NOS isoforms, iNOS, eNOS and nNOS (inducible, endothelial, and neuronal NOS), achieve their key biological functions by tight regulation of interdomain electron transfer (IET) process via interdomain interactions. In particular, the FMN–heme IET is essential in coupling electron transfer in the reductase domain with NO synthesis in the heme domain by delivery of electrons required for O_2 activation at the catalytic heme site. Compelling evidence indicates that calmodulin (CaM) activates NO synthesis in eNOS and nNOS through a conformational change of the FMN domain from its shielded electron-accepting (input) state to a new electron-donating (output) state, and that CaM is also required for proper alignment of the domains. Another exciting recent development in NOS enzymology is the discovery of importance of the the FMN domain motions in modulating reactivity and structure of the catalytic heme active site (in addition to the primary role of controlling the IET processes). In the absence of a structure of full-length NOS, an integrated approach of spectroscopic (e.g. pulsed EPR, MCD, resonance Raman), rapid kinetics (laser flash photolysis and stopped flow) and mutagenesis methods is critical to unravel the molecular details of the interdomain FMN/heme interactions. This is to investigate the roles of dynamic conformational changes of the FMN domain and the docking between the primary functional FMN and heme domains in regulating NOS activity. The recent developments in understanding of mechanisms of the NOS regulation that are driven by the combined approach are the focuses of this review. An improved understanding of the role of interdomain FMN/heme interaction and CaM binding may serve as the basis for the design of new selective inhibitors of NOS isoforms.

Keywords

Nitric oxide synthase; Calmodulin; Electron transfer; Laser flash photolysis; Pulsed EPR; Magnetic circular dichorism

Correspondence to: Changjian Feng.

1. Introduction

1.1. Biomedical significance of nitric oxide synthase (NOS)

Nitric oxide (NO) is a key signaling molecule for vasodilatation and neurotransmission at low concentrations and a defensive cytotoxin at higher concentrations [1, 2]. There are three mammalian NO synthase (NOS) isoforms: neuronal, endothelial and inducible NOS (nNOS, eNOS and iNOS, respectively). For signaling, NO is produced by eNOS in the endothelial cells that line the inner surface of arteries (for blood pressure control), or by nNOS in the brain for nerve signal transduction [3] (nNOS is also present in the peripheral nervous system and muscle tissue). In addition, NO is generated in macrophages by iNOS for immune defense [4–8]. The two constitutively expressed NOS isoforms (cNOS), eNOS and nNOS, are Ca^{2+}-responsive and control basal NO levels, whereas the Ca^{2+}-insensitive iNOS is expressed in response to cytokines or bacterial products. An alternative pathway for NO generation *in vivo* is reduction of inorganic anions nitrate and nitrite. The roles of dietary nitrate [9] and nitrite [10] in cardiovascular health and diseases were recently reviewed.

NO's availability is tightly regulated at the synthesis level by NOS. Aberrant NO synthesis by NOS is associated with an increasing number of human pathologies, including cancer and ischemic injury caused by stroke [2, 11]. Selective NOS modulators are required for therapeutic intervention because of the ubiquitous nature of NO in mammalian physiology, and the fact that three NOS isoforms are each capable of producing NO *in vivo*. Because eNOS is critical for maintaining proper blood pressure, non-selective NOS inhibitors will lead to hypertension. However, it is challenging to design selective NOS inhibitors due to the high active site conservation among the NOS isoforms [12, 13]. Clinical agents that directly and selectively modulate NOS isoform activity remain elusive. Clearly, molecular mechanisms of NOS regulation, once fully understood, will identify key targets for development of *selective* new pharmaceuticals for treating wide range of diseases that lack effective treatments.

1.2. NOS enzymology-Overview

NOS enzymes are monooxygenases, generating NO and citrulline from L-arginine (L-Arg), NADPH and O_2:

$$\text{L-Arg} + 1.5\ \text{NADPH} + 1.5\ H^+ + 2\ O_2 \rightarrow; 1.5\ NADP^+ + \text{Citrulline} + NO + 1.5\ H_2O$$

NOS catalysis is a two-step process (Scheme 1): the substrate, L-Arg, is first converted to N-hydroxy-L-arginine (NOHA), which in turn is converted to NO and citrulline [14, 15]; the nitrogen atom (blue) of NO is from the guanidino group of the L-Arg substrate, and the oxygen atom (magenta) is derived from dioxygen. The monooxygenase reactions are analogous to those of the cytochrome (cyt) P450 systems. The oxidation mechanism of the substrate by NOS heme is intricate, and many details of the catalytic chemistry mechanism remain to be elucidated (as summarized in several recent reviews and articles [15–20]).

Eukaryotic NOS evolved via a series of gene fusion events, resulting in a modular heme- and flavin-containing enzyme that produces NO by tightly controlled redox processes [21]. In contrast to the P450-mediated systems, the flavins and heme cofactors of the NOS are bound to the same polypeptide chain, and the existence of (6R)-5,6,7,8-tetrahydrobiopterin (H_4B) and a coordinated zinc ion set NOS apart from these multicomponent systems. Structurally, mammalian NOS enzyme is a homodimeric flavo-hemoprotein, and each subunit consists of two major domains (Figure 1): an N-terminal catalytic heme-containing oxgenase domain (NOSoxy), which is structurally unrelated to cyt P450s, and a C-terminal flavin-containing reductase domain (NOSred), which is structurally similar to the P450 reductase. NOSred contains ferredoxin-$NADP^+$-reductase (FNR) and FMN modules [22]

and in this way is similar to other NADPH-utilizing dual flavin oxidoreductases [23, 24]. NOSred catalyzes transfer of the reducing equivalents from the two-electron donor NADPH to the heme iron, a one-electron acceptor, where dioxygen is bound and activated. On the other hand, NOSred differs from P450 reductases primarily because of insertions and extensions related to control of NO synthesis (see below). The NOS FMN and heme domains are connected by a calmodulin (CaM) binding linker (Figure 1), occupation of which by CaM is required for electron transfer from the reductase to the oxygenase domain. In Ca^{2+}-independent iNOS isoform, the linker is bound to CaM tightly (but reversibly [25]). In contrast, in nNOS and eNOS the CaM binding is [Ca^{2+}] dependent [21].

The NOS enzyme is active in NO production only as dimer [26] (that forms through the heme domains). The heme does bind to the monomer (there is an iNOS monomer crystal structure [27]), while the heme binding is necessary for dimerization [28]. However the dimer is required for H_4B site formation and other changes that enable substrate bind [29, 30] and allow intersubunit electron transfer from the reductase-domain flavins to the oxygenase-domain heme [31] (see below). Isolated NOS heme domain, but not the flavin domain, dimerizes [32].

NOS holoenzymes and truncated constructs (Figure 1) can be readily expressed in *E. coli.* [33]. The separated domains of the modular NOS protein are active [32, 34], and study of catalytic and electron transfer mechanisms by using the homologous NOS constructs represents a commonly accepted approach in the field [21, 35]. For example, NOSoxy construct has been used to study the oxidative pathways [20], and a bi-domain oxygenase/FMN (oxyFMN) construct is a minimal electron transfer complex designed to favor the interactions between the FMN and heme domains [36].

1.3. Crystal structural characterization of the NOS domains

In 1997, the first X-ray crystal structures of NOS domain were reported [27]. These structures are of monomeric murine iNOSoxy construct lacking the H_4B cofactor and NH_2-terminal residues 77 to 114, and the heme pocket is more exposed in these truncated monomeric structures [27] than in the iNOS dimer [37]. Since then, crystal structures have been reported for the truncated NOS constructs, including the oxygenase domains of each of the NOS isoforms [29, 37, 38], rat nNOS reductase constructs [39, 40], CaM-bound human iNOS FMN domain [41], and CaM bound to peptides corresponding to the CaM-binding region in nNOS (PDB 2O60), iNOS (PDB 3GOF) and eNOS [42]. Getzoff, Poulos, Kim, Crane and their coworkers have been the major contributors to this field. A majority of the structural work to date has been on the heme domains co-crystallized with inhibitors/ligands [13, 43–46]. These structures give considerable insights into the NOS mechanism, and provide a basis for studying structural-functional relationship of the NOS isoforms. Combinations of kinetics, thermodynamics, spectroscopic and crystallographic methods, with site-directed mutagenesis, have given information about the roles of specific amino acid residues in regulating the NOS isoform activity [47–51].

However, the long-standing quest for the structure of a full length mammalian NOS has eluded numerous investigators, probably because remarkable NOS domain motions are involved in the catalysis (see below). Strategies to decrease overall flexibility may help crystallization of the NOS holoenzyme.

1.3.1. Crystal structures of oxygenase domain of NOS—The dimeric oxygenase domain contains an iron protoporphyrin IX. The heme moiety resembles that of cyt P450 in that it has an axial thiolate ligand on the proximal side (Figure 2), and it gives the same type of absorption spectrum when CO binds to ferrous form of heme. The substrate L-Arg and cofactor H_4B both bind near the heme center [37], where the catalytic production of NO

takes place. The oxygenase domain is, however, structurally different from the cyt P450. In contrast to P450 enzymes (where the heme active site undergoes large open/close motions to enable substrate binding and product release) [52], the NOS heme active site is rigid [53] and remains relatively exposed [29]. Beta structure serves as the primary active site architectural motif in NOS, rather than helices as in P450s, giving the rigidity in NOS. The open NOS active site ensures release of the NO product, but the NOS-oxy complex could expose to bulk solvent, resulting in nonspecific protonation that short-circuits the normal reaction path.

To circumvent this problem, the H_4B cofactor near the NOS heme is recruited to give a rapid and coupled electron/proton transfer system, which avoids indiscriminate reaction with bulk solvent. The unprecedented involvement of the H_4B cofactor as an electron donor is unique among P450s and pterin containing proteins. The roles of the H_4B cofactor in iNOS [19, 54, 55], nNOS [56] and eNOS [57] isoforms have thus been under intensive investigations. H_4B promotes dimerization and transiently donates electrons during catalysis [58]. H_4B is also proposed to provide proton(s) during the oxidative chemistry and product release (in the second step of NOS catalysis) [19] processes. Here the timing and source of proton donation is the key to deciding the pathways of substrate oxidative reactions.

Importantly, crystallographic studies have revealed key sites for rational design of selective NOS inhibitors. The high active site conservation among all three NOS isoforms makes the design of selective NOS inhibitors very challenging. Selective NOS inhibitor is not available for clinical usage. Not until recently, by using a combination of crystallography, computational methods and site-directed mutagenesis, it was found that inhibitor chirality and an unanticipated structural change of the target NOS enzyme control both the orientation and selectivity of nNOS inhibitors [13, 59]. Another crystal structural and mutagenesis study identified an induced-fit binding mode linking a cascade of conformational changes to a new specificity pocket [45]. Here enzyme elasticity of an isoform-specific triad of distal second- and third-shell residues modulates conformational changes of conserved first-shell residues to decide the inhibitor selectivity.

Recently, micro-spectrophotometric techniques have been used to confirm redox state of the NOS heme center and the status of diatomic ligand (CO/NO) complexes during X-ray diffraction data collection [60]. This technique is of great potential in observing the X-ray-induced reductions in the redox-sensitive heme cofactor.

1.3.2. Crystal structures of reductase domain of nNOS—The first structure of NADPH/FAD-binding domain of rat nNOS (in complex with $NADP^+$) revealed interesting similarities and differences compared to P450 reductase [39]. Soon afterward an intact CaM-free nNOS reductase domain structure was solved [40]. The position and conformation of key parts of the NOS-specific regulatory elements, including the autoregulatory (AR) insert within the FMN subdomain and the C-terminal tail (CT), were revealed by this structure [40] (Figure 3). Specifically, part of the AR insert forms a helix connecting the FMN and NADPH/FAD binding domains by hydrogen bonds. This supports an effect of AR on the domain alignment. About half the AR is disordered in this structure. In addition, CT lies at the interface between the FMN and FAD subdomains, and its position indicates that the CT helix restrains the FMN module from moving away from the FNR module, thus stabilizing the FMN-shielded conformation. However, the terminal 16 residues are not observable, suggesting flexibility in this region of CT. Conformational diversity in NOSred is also evident from weakly defined electron density for parts of the connecting domain (CD), including the hinge linking the FMN domain to the CD, and the β-finger containing the CD2A regulatory element (which contributes to the observed cNOS Ca^{2+}/CaM dependence

by interacting with the CaM-binding linker [61]). Rotational flexibility of the FMN domains is also observed.

The FMN and FAD isoalloxazines are in close contact (the FMN isoalloxazine is located within 5 Å of the FAD isoalloxazine in an edge-on configuration) [40], while FMN is inaccessible to exogenous redox partners. It is difficult to visualize a conformation in which FMN is in contact with both FAD and heme. Requirements for electron tunneling and constraints imposed by docking crystallographic structures indicate that catalytically competent electron transfer from FMN to heme cannot occur in the reductase conformation observed in the crystal structure [40].

1.3.3. Crystal structures of CaM-bound NOS peptides and domains—The crystal structure of CaM bound to a 20-residue peptide comprising eNOS CaM-binding region establishes their individual conformations and intermolecular interactions, and suggests the basis for isoform-specific differences [42]. Upon CaM binding to eNOS/nNOS, a major conformational change occurs in the CaM structure, forming a ‘latch' over the CaM-binding NOS sequence (Figure 4) [42]. The latch domain, composed of regions from the Ca^{2+}-binding motifs EF hands 1 and 3, is critical in eNOS/nNOS activation by CaM [62, 63]. CaM phosphorylation at the latch domain (e.g. Ser101) may represent a unique pathway in the regulation of eNOS activity, and thereby may play an important role in modulating NO-mediated vascular responses [64].

Regarding the NOS regions involved in activation by CaM binding, it is clear that interaction with the canonical CaM-binding site (yellow chain in Figure 4) is insufficient for NOS activation [65], and the exterior regions of bound CaM may also interact with the eNOS/nNOS domains. For example, specific AR regions in the FMN domain are likely to be well positioned to interact directly with the CaM exterior [66]. Direct interaction of the AR with CaM was recently proposed by Masters lab to be important for the stabilization of the “open” complex [67].

While the sites of inter-protein interactions between CaM and the CaM-binding linkers of eNOS [42], nNOS (PDB 2O60) and iNOS (PDB 3GOF) have been resolved, there is only one structure for CaM in complex with the FMN domain of human iNOS [41]. In this structure the CaM-binding region together with CaM forms a hinge and pivots on the R536(NOS)/E47(CaM) pair (Figure 5); note that R536 at the end of the CaM-binding region is conserved in the NOS isoforms and is the only residue that interacts with both the CaM and the FMN domain. This CaM/NOS hinge is predicted to regulate the electron transfer from FAD to FMN and from FMN to heme by adjusting the relative orientation and distance among the three cofactors [41]. Indeed, kinetic studies of nNOS mutants at the conserved arginine [68, 69] demonstrate that the Arg(NOS)-Glu(CaM) bridging interaction (Figure 5) is the key feature that enables CaM to activate nNOS.

How surfaces of CaM interact with the NOS domains remains enigmatic, and is mechanistically important in CaM-regulated NOS function. The CaM-binding to NOS and the CaM-dependent activation of the NOS enzymes have been under intensive investigation. A variety of CaM mutants [70–72] and chimera [65] were constructed to study the effects of specific CaM regions/residues on the different electron transfer steps in the NOS enzymes. Interestingly, an elegant approach was used to separately measure Ca^{2+} concentration required for CaM to bind and activate eNOS [73, 74]. Fluorescence and Förster resonance energy transfer were recently applied to monitor the orientation and conformation of CaM when bound to the NOS peptides and enzymes [75, 76]. Based on these kinetics and spectroscopic results, a sequential CaM binding model was proposed, in which CaM binds to the cNOS enzymes with the Ca^{2+}-replete C-lobe binding first followed by the Ca^{2+}-

replete N-lobe [76, 77]. On the other hand, the iNOS isoform has a distinctly different mechanism: both the N- and C-terminal EF hand pairs bind to the iNOS peptide in a Ca^{2+}-independent manner, but only the C-terminal domain showed notable Ca^{2+}-dependent conformational changes when associated with the target sequence [75]. It is important to further measure the dynamic conformational changes of CaM in complex with the NOS isoforms and their modified forms such as phosphorylated NOSs (that are directly relevant to biological functions).

1.4. Major breakthroughs in NOS enzymology

In the past decades, significant advances in NOS enzymology have taken place in several important aspects. These include, but are not limited to, the following:

1. Identification of nNOS [78] and iNOS [79] as a P450-like heme-thiolate protein in 1992.
2. High-level expression of functional nNOS [33, 80], eNOS [81] and iNOS [82] proteins around 1995. This is critical for growing protein crystals, studying key NOS forms by advanced spectroscopic techniques, and investigating roles of specific residues in NOS function.
3. Reports of X-ray crystal structures of oxygenase domain of iNOS [37] and eNOS [29] isoforms in 1998.
4. Discovery of intrinsic control elements in NOS reductase domain by Masters, Salerno, Gross and coworkers (reviewed in ref. [21]).
5. Discovery of the role of H_4B in NOS electron transfer and catalysis by Marletta and coworkers around 1999 [58]. Vasquez-Vivar *et al.* further showed that H_4B is important in the coupling/uncoupling of NOSs to form either NO or superoxide [57, 83].
6. A global catalytic model that highlights the role of NO as an intrinsic regulator was proposed by Stuehr and coworkers in 2001 [84]. Based on this NO-inhibition mechanism, a pulsed NO-production model of nNOS at 37 °C was proposed by Salerno in 2008 [85].
7. NADPH-lock model proposed by Daff in 2002 [86].
8. Over the past 10 years, a few NOS homologs have been identified and characterized in a number of mostly Gram-positive bacterial species [87, 88]. Exciting developments in bacterial NOS have been summarized in an excellent review by Crane [89]. In contrast to mammalian NOSs, which possess both a catalytic heme and a reductase domain, most bacterial enzymes lack reductase domains and require the supply of external redox partners to support NO production [90]. However, Marletta lab recently identified a catalytically self-sufficient bacterial NOS that also contains a fused reductase domain [91]. Despite some interesting differences in cofactor utilization and redox partners, the bacterial NOS enzymes are in many ways similar to their animal NOS counterparts. As such, studies of the bacterial NOSs [92–94], in particular of their especially stable oxy-heme complexes [18, 95], have provided insight into the structural and catalytic properties of the NOS family.

Several seminal reviews on NOS mechanism have recently been published [14, 15, 21, 96, 97]. Dr. Bettie Sue Masters published an article entitled *A Professional and Personal Odyssey* [98], which summarizes the research on NOS biochemistry both scientifically and historically. In this article, Dr. Masters writes “I suppose one could summarize my approach to science as one in which we ask questions that we think are important to answer and then

determine the approaches, methodological, technological or intellectual, to be applied to answer these questions" [98]. It is of our hope that the present review will convey the same message by discussing the importance of the mechanistic questions to be addressed, and describing how specific experimental approaches can be utilized to tackle the problems.

The scope of this review is primarily about roles of electron transfer and interdomain interactions in NOS isoform regulation. We will first briefly review the thermodynamic, rapid kinetics, and spectroscopic approaches in studying discrete interdomain electron transfer (IET) processes in the NOS enzymes. We will focus on the laser flash photolysis approach we developed for direct determination of kinetics of the IET between the FMN and Fe centers. Spectroscopic studies of the IET-relevant NOS forms/intermediates will also be discussed; a focus will be on recent pulsed electron paramagnetic resonance (EPR) studies. We will then review the current understanding of the NOS FMN–heme IET mechanism, followed by discussion of recent kinetics and spectroscopic studies that demonstrate new roles of docked FMN domain in NOS function. Finally, we will discuss future directions addressing vital mechanistic questions in this field.

2. The interdomain electron transfer in NOS regulation

Although many details of the novel NOS catalytic mechanism remain to be elucidated [97, 99], it is well accepted that IET processes from NADPH to heme through FAD and FMN (Figure 6) are key steps in NO synthesis through coupling reactions in the domains [14, 21, 100]. Tight coupling of the IET processes in NOS enzyme is important for normal physiological function and prevention of disease, because uncoupled or partially coupled NOS results in deleterious effects (via production of excessive reactive oxygen species) [57, 101, 102]. Therefore it is of current interest to study the NOS IET control mechanism.

The flavin cofactor can exist as the fully oxidized (ox), the one-electron reduced semiquinone (sq), or two-electron fully reduced hydroquinone (hq). The NOS flavin semiquinone radical is neutral, based on the blue color [103] and EPR measurements [104, 105]. FMNH• and FADH• are thus shown for the semiquinone forms in the cycle (Figure 6). On the other hand, the protonation state of the flavin hydroquinone is not known yet, and FMN_{hq} and FAD_{hq} are used to represent FMN hydroquinone and FAD hydroquinone, respectively. In NOS the sq/hq redox potential of FMN is lower than that of the ox/sq couple [106] and hence it is the FMN_{hq} form that delivers electrons to the heme.

The electron source is NADPH, which donates two electrons to FAD (through a hydride transfer) (Figure 6). This is followed by the IET from the FAD_{hq} to FMN [107, 108]. The FMN domain containing FMN_{hq} is then proposed to move away from the FNR module to transfer electrons to the ferric heme in the oxygenase domain. Unlike iNOS, eNOS and nNOS synthesize NO in a Ca^{2+}/CaM dependent manner (Figure 6): CaM-binding (induced by an influx of Ca^{2+}) enhances the IET reaction from the FAD_{hq} to FMNH• (reaction 1) [49], and triggers the IET from the FMN_{hq} to the catalytic heme iron in the oxygenase domain of another subunit (reaction 2) [31, 48, 109, 110]. CaM binding has little effect on the thermodynamics of redox processes in NOS [106, 111, 112]. CaM binding was also reported to substantially shift redox potentials of flavin cofactors in an NOS reductase construct [113]. Nonetheless, it is generally accepted that the regulation by CaM is accomplished dynamically through controlling redox-linked conformational changes required for effective IET.

The repression of cNOS electron transfer, and its relief by CaM, involves intrinsic control elements in the reductase domain [21]. Analysis of protein sequences and related mutagenesis studies show that the cNOS reductase domain has at least three control elements which are not present in P450 reductase [21]. They are an AR insert (~ 40 amino

acids) in the FMN domain [66, 114], a short insert in the connecting domain between the FAD and FMN domains [61], and a CT (Figure 3) [115, 116]. Note that the AR insert only exists in nNOS and eNOS, but not in iNOS, and that the size of the CT is different in the three NOS isoforms. Control elements deletion studies indicated that they repress electron flow into and out of the NOS reductase domain in the CaM-free state, and may help to relieve the repression upon CaM binding [115–120]. It has been shown that the control elements regulate the IET in a concerted manner [61, 66, 114–116]. A recent crystal structure of an intact, CaM-free nNOS reductase has revealed key information about how certain control elements may repress electron transfer [40] (as discussed in Section 1.3.3 above). Extrinsic posttranslational modifications to the control elements, including phosphorylation at the AR and CT sites, as well as inter-protein interactions, are important in NOS regulation in cellular environment (reviewed in ref. [21]). Biochemical studies of the phosphomimetic mutants in eNOS C-terminal tail provided rationale for "calcium-independent" eNOS activation by phosphorylation [121]. These extensive studies have established a basic framework for regulation of IET in the NOS domains. Here utilization of appropriate experimental approaches (as detailed below) is critical for studying the IET mechanism.

2.1. Experimental approaches in studying the IET mechanism

In addition to molecular biology and protein crystallography, there are three major types of techniques in studying the NOS IET mechanism: thermodynamics, rapid kinetics and spectroscopic approaches (including MCD [122–124], resonance Raman [125], NMR [126], X-ray absorption spectroscopy [127], and EPR [50, 105, 128]). The approaches are briefly described below. Of the spectroscopic methods, we will only discuss pulsed EPR techniques. Applications of resonance Raman to the NOS problems have been recently reviewed by Rousseau and Yeh [129]. Interestingly, resonance Raman spectroscopy combined with a continuous-flow rapid solution mixer was used to study the structural properties of the metastable dioxygen-bound complexes of iNOSoxy [20].

The intersubunit FMN–heme IET (reaction 2, Figure 6) is essential in coupling electron transfer in the reductase domain with NO synthesis in the heme domain by delivery of electrons required for O_2 activation at the catalytic heme site [31]. A combined laser flash photolysis and pulsed EPR approach (Figure 7) is recently developed in laboratories of Feng, Tollin and Astashkin. This new integrated approach is powerful in studying molecular mechanism of the FMN–heme IET. Pulsed EPR techniques that can be used are: (i) relaxation-induced dipolar modulation enhancement (RIDME), (ii) electron-electron double resonance (ELDOR), (iii) electron-nuclear double resonance (ENDOR), and (iv) electron spin echo (ESE) envelope modulation (ESEEM); they represent powerful tools for studying the structure and function of paramagnetic centers (such as metal ions) in biological systems [130]. The focuses of this section are thus on: (i) the new CO photolysis approach (for direct determination of the FMN–heme kinetics), and (ii) RIDME technique in determination of the distance between the FMN and heme centers in NOS. Table 1 summarizes the information content of these techniques, and how they can provide key information regarding the NOS regulation mechanism as it relates to interdomain FMN–heme interactions. All the data collectively can be used to directly test hypothesis and working model on critical structural determinants in modulating the IET in NOS.

2.1.1. Thermodynamic approaches

It is important to determine midpoint potentials (Em, the driving force required for electron transfer) of the redox centers (FAD, FMN and heme) in NOS. To date, there are three major approaches to determine the Em: redox titration (using sodium dithionite as the reductant and potassium ferricyanide as the oxidant) [106, 113], spectroelectrochemistry [131], and

protein film voltammetry [132]. In the first two approaches, titrations are generally monitored *in situ* optically with a UV-vis spectrophotometer, or by measuring EPR spectra of samples withdrawn from the cuvette at certain solution potentials [113]; mediators are added to facilitate electron transport between enzyme and electrode [133]. The electrochemistry of H_4B in solution was also re-visited [134].

Substrate binding to NOS does not induce significant increase in redox potential of heme [135], which is in contrast to P450 enzyme where the substrate binding causes a notable increase (thereby facilitating heme reduction in P450). It is also of note that heme midpoint potentials in the absence of H_4B and substrate have been determined to be −347 mV and −239 mV for iNOS and nNOS, respectively, and these values shift to −263 mV and −248 mV when H_4B and L-Arg are both bound within the respective enzyme's active site [136]. Even though iNOS and nNOS both contain the same general structure and have the same catalytic function, this variance in heme midpoint potential in the absence of H_4B and substrate (−347 mV vs. −239 mV) reveals some notable dissimilarities between the two isozymes, which merits further investigations.

Isothermal titration calorimetry was recently used to measure the thermodynamics of cofactor binding to the isolated reductase domain of nNOS and its mutants, and the results suggested conformational rearrangements induced by the cofactor binding to NOS [137].

2.1.2. Rapid kinetics approaches-Overview

The following steady-state kinetics assays have been used to measure NOS holoenzyme activities: (i) NO formation by hemoglobin capture assay [138]; (ii) cyt *c* reduction activity, a measure of the release of the FMN domain from the reductase complex [65]; and (iii) NADPH oxidation and ferricyanide reduction activities, measure of IET rates into and out of FAD domain, respectively [67]. Activity assay of truncated NOS domain requires additional treatments (e.g. H_2O_2-supported oxidation of NOHA [36], pre-reduction of NOSoxy construct). This is due to lack of endogenous electron transfer partners in the truncated constructs.

Stopped flow has been utilized to determine kinetics of discrete IET steps during NOS catalysis. Typical examples are: (i) determination of the IET kinetics between the flavins [139]; (ii) anaerobic pre-steady-state cyt *c* reduction [140]; (iii) anaerobic heme reduction [141]; (iv) anaerobic flavin reduction (monitored by absorbance changes at 458 and 600 nm [142], and by fluorescence and transient spectra [108]); and (v) study of H_4B radical formation [143].

Along with the single-turnover stopped flow experiments, the use of cryogenic spectroscopic technique has been critical in revelation of the role of H_4B as a one-electron donor to NOS [Fe(II)−O_2] heme, an intermediate in the catalytic cycle [144]. The low temperature technique slows the rate of reaction of ferrous NOS with O_2 by lowering the reaction temperature to subzero values. This not only reduces the rate to such an extent that the reaction can be followed on a time scale from seconds to minutes, but also allows observation of intermediates that do not accumulate at higher temperatures [144]. The freeze-quench technique was used to study the redox reactions between heme and H_4B in NOS [145–147]. Interestingly, Stuehr and coworkers utilized an EPR method to separately quantify the flavin and pterin radicals in NOS reactions [145], and the results showed that the NOS flavin domain facilitates reduction of the pterin radical following the L-Arg hydroxylation [145].

2.1.3. Rapid kinetics approaches-Laser flash photolysis

Laser flash photolysis is another powerful rapid kinetics technique in studying discrete steps in NOS catalysis, and the applications include measurement of: (i) kinetics of CO/NO binding to NOS heme [148–151]; (ii) photoreduction of NOS by rhenium(I)-diimine wires [152]; (iii) photoinitiation of NOS activity by a NADPH substitute [153, 154]; and (iv) direct determination of the FMN–heme IET by a new CO photolysis approach developed in the laboratories of Feng and Tollin [155–159].

The CO photolysis approach (Figure 8) can be used to measure precisely kinetics of the FMN–heme IET step, and is briefly described as follows. All the experiments are conducted in dark. A solution containing 5-deazariboflavin (dRF) and fresh semicarbazide in buffer is vigorously degassed in a laser photolysis cuvette by a mixture of CO and Ar (with a volume ratio of ~ 1:3). The mixed gas passes through an oxygen-removing column and a water-containing bubbler (to saturate the gas with water) before entering the cuvette (Figure 9a). Aliquots of concentrated NOS protein are subsequently injected through a septum to achieve the desired concentration, and the protein solution is kept in ice and further purged by passing the CO/Ar mixture over the solution surface for 60 min (Figure 9a). This is to remove minor oxygen contamination in the aliquots (before being mixed into the buffer and subjected to illumination). Incubation of the whole cuvette in ice (Figure 9a) helps removal of oxygen and stabilization of the protein during the long purging process. Particular care is needed to avoid bubbling of the protein sample. It is critical to well degas the buffer and protein aliquots because oxygen readily reacts with Fe(II) NOS.

The protein solution in the cuvette is then illuminated for an appropriate period (minutes) by a white light source to obtain a partially reduced form of NOS [Fe(II)–CO][FMNH$^{\bullet}$]. It is best to incubate the sample cuvette in ice before and after the illumination, which helps (i) better control of the photoreduction extent and (ii) stabilize the protein. The sample is subsequently flashed with a 446 nm laser excitation (Figure 9b) to dissociate CO from Fe(II)–CO to generate a transient Fe(II) species that is able to transfer one electron to the FMNH$^{\bullet}$ to produce FMN_{hq} and Fe(III). This IET process can be followed by the time-resolved loss of absorbance of FMNH$^{\bullet}$ at 580 nm or loss of absorbance of Fe(II) at 465 nm for iNOS [155] or 460 nm for nNOS [156] (Figure 8). Typical kinetics traces are shown in Figure 10. Upon a laser excitation, the absorption at 580 nm decays below the pre-flash baseline (Figure 10a), which is due to the FMN–heme IET resulting in FMNH$^{\bullet}$ depletion (eq 1) [155], followed by a slower recovery toward the baseline (Figure 10b), which is due to the CO rebinding to Fe(II).

$$[Fe^{II}][FMNH^{\bullet}] \rightleftharpoons [Fe^{III}][FMN_{hq}] \quad \text{(eq 1)}$$

Since the IET reaction is an equilibrium process, it is in fact measured in both directions; the CO photolysis technique follows the IET process in the reverse direction of the enzymatic turnover. Importantly, the rate constant of the rapid decay (Figure 10a) is independent of the signal amplitude, *i.e.* reduced protein concentration, confirming an intra-protein process.

Heme reduction in NOS isoforms was also indirectly probed by formation of the Fe(II)-CO complex using a stopped flow approach at 10 °C [141]. However, this approach was unable to distinguish the CO binding and heme reduction reactions, as only formation of the Fe(II)-CO complex was observed. Thus the CO photolysis approach offers clear advantages since it allows us to observe both processes directly. Note the spectroscopic “transition” (*i.e.* a reversal in direction of absorption changes over time) in the 580 nm traces (inset of Figure 10b).

Research-grade laser flash photolysis apparatus is commercially available through several manufacturers, including Edinburgh Instruments and Applied Photophysics. For most of the standard setups they offer, there is only one monochromator after the sample holder, and a Xe arc lamp is provided. This lamp is generally not ideal for long time scale (ms to seconds) measurements due to stability issue. It is better to have another halogen lamp installed (Figure 9b), which is much more stable at the long time scale (albeit not that bright). Additionally, a LVF-HL adjustable-pass filter (Ocean Optics Inc.) with band pass peaked at selected wavelength (e.g. 580 nm) should be placed in between the light source and the protein sample (Figure 9b) to minimize potential photo-bleaching and further photo-reduction by the white monitor beam.

Some additional features of the methodology are also worthy of note.

1. The laser-irradiated volume in the sample cuvette is kept small (< 1% of the total volume) so that only minor net photo-induced conversion occurs. This allows the sample to be subjected to multiple flashes for signal averaging. Here the laser focusing and alignment of the laser and monitor beams are critical (Figure 9b). A cuvette holder with optical ports and pinholes, such as TLC 50 by Quantum Northwest, is useful to assist the alignment and protect the sample from ambient lights. The alignment is also important for better signal-to-noise ratio.
2. A key control experiment is that traces with different signal amplitudes are always collected [159]. If the traces give similar rates, the electron transfer process is of an intra-protein nature. This is important because other inter-protein processes may confound the absorption changes, and if so, the observed rate would depend upon protein concentration. Therefore, the kinetics must be determined at various protein concentrations to confirm that the intra-protein electron transfer process between the FMN and Fe centers is being measured.
3. It is pivotal to generate sufficient amounts of [Fe(II)-CO][$FMNH^{\bullet}$] by the photochemical reduction. Proper dRF concentration and illumination duration are two key factors for reducing FMN to $FMNH^{\bullet}$, but not for further reducing $FMNH^{\bullet}$ to FMN_{hq}. Pre-cooling of the sample (in ice) is also necessary to control the reduction extent. It is very important to degas the buffer and protein aliquots for sufficient time before the illumination (see above).

2.1.4. EPR approaches

The NOS forms/intermediates studied by EPR include: high-spin ferric heme center of the NOS isoforms [128, 160, 161], cryoreduced high valence oxy-NOS [18, 162], H_4B radical [19, 54], $FMNH^{\bullet}$ radical [105] and low spin ferric heme/$FMNH^{\bullet}$ form [163]. Spin-trapping is a powerful approach to directly probe NOS-produced reactive oxygen species [56, 57, 101, 164].

EPR has been used for detailed structural determination of the NOS enzymes. Dr. Brian Hoffman and his colleagues pioneered in using ENDOR to determine the location of the guanidino nitrogen atom of L-Arg. The obtained distance value is in excellent consistent with the crystal structure [128]. This was the first demonstration of the proximity of the reactive guanidino nitrogen of L-Arg to heme iron, before the crystallographic data were available. A difference of only 0.06 Å between the iNOS and nNOS isoforms was detected by the ENDOR measurements [160].

The structural basis for the assembly of the NOS domains and CaM during catalysis is poorly understood, as crystal structures are only available for truncated NOS domains [29, 37–42, 45]. Trying to piece together the heme and reductase domain structures by

computational docking studies may provide some insights [35, 41], but alternative models will be difficult to distinguish when compared to the favored ones. Therefore, it is important to utilize pulsed EPR methods that can provide distance constraints within the FMN–heme IET complex. The FMN···Fe distance information is also important for better understanding the FMN–heme IET mechanism, because the distance and orientation between redox centers is critical for controlling electron transfer processes in proteins [165].

In general, the magnetic dipole interaction between two paramagnetic centers, D, is directly related to the inter-spin distance, R ($D \propto R^{-3}$), and pulsed EPR approaches utilizing this fact have been used to determine the inter-spin distances in biological systems [166–168]. Therefore, one can use the pulsed EPR techniques of RIDME [163] and pulsed ELDOR [169] to study NOS forms containing paramagnetic Fe and FMN centers, such as the NOS [Fe(III)][FMNH$^{\bullet}$] form. Moreover, FMN and heme are native cofactors in NOS, and their mutual orientation, as well as their orientation with respect to the dipolar vector $\boldsymbol{r}$, are constrained by covalent or hydrogen bonds. Pulsed EPR can provide *detailed* structural information: mean distance, orientation of the radius-vector $\mathbf{R}_{\mathbf{Fe\text{-}FMN}}$ joining the heme and FMNH$^{\bullet}$ centers, and relative orientation of the heme and FMNH$^{\bullet}$ molecular frames (see below). The results can thus provide unique insight into the FMN/heme alignment and possibly reveal the FMN domain motions during NOS catalysis. This information is directly relevant to the efficiency of the FMN–heme IET and the bioactivity of NOS isoforms.

The NOS FMNH$^{\bullet}$ is an organic radical that has a rather narrow EPR spectrum (~2.5 mT wide) and sufficiently long longitudinal and transverse relaxation times that make its ESE signal easily observable at moderately low temperatures (tens of Kelvin) [163]. For the Fe(III) center two possibilities were considered. The high-spin (S = 5/2) ferric heme has an extremely broad EPR spectrum characterized by $g_{\perp} \sim 6$ and $g_{//} = 2$, and its magnetic relaxation time is usually too short for any meaningful pulsed EPR measurements even at 4.2 K. On the other hand, low-spin (S=1/2) ferric heme (excluding the so-called high anisotropy low-spin centers) has a significantly narrower EPR spectrum (usually confined between g ~ 3 and g ~ 1.4), and has sufficiently long magnetic relaxation time to be easily detected by pulsed EPR at temperatures below 15 K. Therefore, for the pulsed EPR measurements, the NOS protein samples containing low-spin heme, as opposed to high-spin heme, are selected [163]. The heme can be converted to exclusively low-spin form with addition of imidazole that binds directly to the heme iron.

For preparation of the [Fe(III)][FMNH$^{\bullet}$] sample, the as-isolated NOS sample is anaerobically titrated by dithionite to partially reduce the protein, which is monitored carefully by absorption spectra [163]. Importantly, optimal conditions for making the [Fe(III)][FMNH$^{\bullet}$] sample in which the two paramagnetic centers reside in the same protein molecule have been identified [163]. Ethylene glycol (40%) is added into the sample (as a cryoprotectant) to form a homogenous glassy sample and to minimize spectroscopic diffusion effects. This reagent was also used in low temperature MCD [170, 171] other pulsed EPR [18, 162] studies of NOS proteins.

For transferring the sample into an EPR tube (X- or Ka band), a polyethylene (PE) tubing is securely attached to a pipette tip (to be used along with a piston-driven air displacement pipette). The tubing is cut to be a bit longer than the height of EPR tube. A single channel pipette is set at the desired sample volume (~ 60 and 30 μl for X- and Ka band EPR tubes, respectively), and is used to transfer a measured volume of protein sample into bottom of the EPR tube (through the PE tubing). The advantages of transferring samples in this way include: (1) a set volume of protein sample is readily transferred and loss of precious protein sample is minimal; (2) PE tubing is much better than glass pipette for transferring, as it does not break inside the EPR tube, is flexible (so it is easier to operate) and has different sizes

(for fitting into different EPR tubes); (3) the protein sample does not stick to the PE surface that much; and (4) potential operational mistake is minimized.

RIDME technique [172] was then used to measure the ESEEM caused by the dipole interactions between the paramagnetic FMN and heme iron centers in the [Fe(III)][FMNH$^{\bullet}$] form, from which the FMN···Fe distance in a human iNOS oxyFMN construct has been evaluated (Figure 11) [163]. This RIDME study is the first of its kind to be performed on a NOS protein. In the RIDME experiments, a refocused stimulated ESE signal of the FMN radical is observed, while the longitudinal relaxation of the heme Fe(III) center serves the purpose of modifying the local magnetic field for the radical spin. The dipolar ESEEM (whose amplitude is temperature-dependent) can be separated from nuclear ESEEM (that is temperature-independent) by dividing the RIDME trace recorded at 15 K by that obtained at 25 K. This is based on the fact that only about 40% of the NOS Fe(III) spins have a chance to flip within the relaxation interval T of 20 μs, whereas at 25 K the dipolar ESEEM has a maximum amplitude because all the Fe(III) spins had flipped at least once [163].

The 18.8 Å distance obtained [163] is in excellent agreement with the IET rate constants [155]. The orientation of the Fe – FMN radius-vector, $\mathbf{R}_{\mathbf{Fe\text{-}FMN}}$, with respect to the heme g-frame was also determined from simulation of the RIDME spectra [163]. Additionally, ENDOR spectra of the deuterons at carbons C2 and C5 in the deuterated coordinated imidazole were obtained to determine the relative orientation of the NOS heme g- and molecular frames, from which $\mathbf{R}_{\mathbf{Fe\text{-}FMN}}$ can be referenced to the heme molecular frame [173]. Numerical simulations of the ENDOR spectra showed that the g-factor axis corresponding to the low-field EPR turning point is perpendicular to the heme plane, while the axis corresponding to the high-field turning point is in the heme plane and makes an angle of about 80 degree with the coordinated imidazole plane [173]. The selected heme-FMN domain docking model (Figure 11) [163] is in qualitative agreement with the experimental results of the pulsed EPR works [163, 173].

2.2. Mechanism of the FMN–heme IET in NOS

2.2.1. FMN-domain tethered shuttle model

A tethered shuttle model (Figure 12) was proposed by Ghosh and Salerno [174], and supported by kinetics [35, 140, 155–159, 175–177] and thermodynamic [137] studies. This model is similar to that of NADPH-cytochrome P450 reductase and P450 BM3, which came out years earlier and derives from P450 reductase [24, 178] and P450 BM3 structures, including the crystal structure of the BM3 heme-FMN complex [179]. The crystal structures of NADPH cytochrome P450 reductase implies that a large domain movement is essential for electron transfer from NADPH via FAD and FMN to its redox partners [180] and cofactor binding [181]. Furthermore, the ancestral electron transfer systems (e.g., flavodoxin/flavodoxin reductase) operate with flavodoxin as a shuttle between the two-domain reductase and other components. In a modular enzyme of NOS containing the domains derived from these ancestors, a tethered shuttle still operates, with the tethers corresponding to the FMN-oxygenase and FAD-FMN connectors (Figure 12). The novel aspect of NOS, of course, is the involvement of CaM. Here CaM activates NO synthesis in eNOS and nNOS through a conformational change of the FMN domain from its shielded electron-accepting (input) state to a new electron-donating (output) state [96, 157, 176, 177, 182]. In the two states, the FMN domain is engaged in distinctly different interdomain interactions, and the module swings back and forth to contact the FNR module and the NOS heme domain (Figure 12). Based on the crystal structure of an intact reductase domain, a similar docking model was proposed by Garcin *et al.* [40].

Crystallographic studies of the NOS reductase unit [40] and of the homologous NADPH P450 reductase [24] have revealed a structure in which the flavodoxin-like FMN binding domain is tightly associated with the flavodoxin-NADPH reductase-like two-domain C terminal unit, forming a complex in which electrons can readily pass from NADPH to FMN through FAD (Figure 3). However, in this conformation the FMN cofactor is inaccessible to the heme of the oxygenase domain, as the oxygenase heme could not be docked within 25 Å of the FMN in the reductase structure [174]. The tethered shuttle model (Figure 12) thus involves an input state corresponding to the existing intact reductase structure [40] (*i.e.* docked FAD/FMN state), and an output state in which the FMN binding domain associates with the oxygenase domain (*i.e.* docked FMN/heme state). Free FMN domain conformations may also exist in between these two docked states. The structure of the functional output state has not yet been determined. To favor observation of the output state, bi-domain NOS oxyFMN constructs, in which only the oxygenase and FMN domains, along with the CaM binding region, are expressed (Figure 1), were recently designed and constructed [35, 36, 183]. Biochemical, kinetics and spectroscopic results have shown that these homologous dimeric oxyFMN constructs are validated models of the NOS output state for NO production [36, 158, 159, 171]. One can argue that the results obtained from the bi-domain oxyFMN system may not be fully applicable to holo-NOS. However, utilization of a similar bi-domain construct of P450 BM3 yielded results that were helpful in understanding the full-length enzyme [179, 184].

The FMN–heme IET kinetics in a rat nNOS holoenzyme [157], and in murine and human iNOS holoenzymes [155] have been directly measured by laser flash photolysis. The IET kinetics for the NOS holoenzymes are approximately an order of magnitude slower than the corresponding NOS oxyFMN constructs. This fact suggests that in the holoenzyme the rate-limiting step in the IET reaction is the conversion of the input state to the output state (in which the FMN becomes accessible to the heme), and that the role of CaM is to allow this conversion to occur. The observed IET rate may thus be the same as the conformation conversion rate. Interestingly, the IET rate constant of eNOS holoenzyme is about ten times smaller than those of both nNOS and iNOS holoenzymes, and a slower conformational change is most likely the cause of the slower IET in eNOS [185].

Importantly, an appreciable decrease in the FMN–heme IET rate constant value of a human iNOS oxyFMN construct was observed with an increase in the solution viscosity [186]. The IET rate constant is inversely proportional to the viscosity for both viscosogens (ethylene glycol and sucrose). The dependence of IET can be explained by the following mechanism (also see Figure 13),

$$[\mathrm{Fe^{II}}][\mathrm{FMNH^{\bullet}}]_{\mathrm{NR}} \underset{k_{-1}}{\overset{k_1}{\rightleftharpoons}} [\mathrm{Fe^{II}}][\mathrm{FMNH^{\bullet}}]_{\mathrm{R}}$$

$$[\mathrm{Fe^{II}}][\mathrm{FMNH^{\bullet}}]_{\mathrm{R}} \underset{k_{-2}}{\overset{k_2}{\rightleftharpoons}} [\mathrm{Fe^{III}}][\mathrm{FMN_{hq}}]$$

which shows two conformationally different precursors, being designated NR (for electron transfer non-reactive) and R (for electron transfer reactive), respectively. A significant increase in the fluorescence intensities with the added solvents was also observed [186]. This indicates that the FMN domain stays in the docked FMN/heme state transiently, and the interdomain FMN/heme docking is retarded by increased viscosity, resulting in less percentage of the docked FMN domain conformation in the sample (*i.e.* less FMN fluorescence quenched by the proximal paramagnetic heme center). The IET kinetics and NOS flavin fluorescence results can thus be considered as new evidence that the observed IET rate is not due to the intrinsic electron transfer process, but rather is gated by a large

conformational change (Figure 13), presumably mediated by the CaM-binding linker (that joins the FMN and heme domains) [186]. Indeed, four conformations in the crystal structure of CaM-bound iNOS FMN domain indicate the FMN domain movements in electron transfer (to fine tune the distance and orientation between the redox centers) [41]. Note that the CaM-binding step is omitted in Figure 13 because it is rapid [187] and should not be rate-limiting in the IET process.

In line with the tethered shuttle model, Daff recently proposed several mechanisms [17] that can limit the FMN–heme IET: (i) the conformational change is slow and thus gates the IET; (ii) the enzyme may spend only a small percentage of time in the docked state; and (iii) the intrinsic rate constant may be slow in the docked output state due to imperfect alignment. The viscosity work clearly demonstrates that factor (i) is responsible for the viscosity-retarded IET kinetics [186]. Additionally, it is likely that the docked state is populated only transiently [35, 96], and the fluorescence results appear to support such a mechanism in which increased viscosity lowers the percentage of the docked FMN/heme conformation [186]. To date, it is difficult to quantitate the FMN domain conformational equilibrium in Figure 13. A promising approach is determination of the NOS flavin fluorescence lifetime, which may provide insight into the dynamics of the FMN domain conformational change [188]. It is also of urgent need to carry out detailed studies of the relative alignment of the NOS FMN and heme domains (including the mean FMN···Fe distance, the relative orientation of the FMN and heme centers, and the distance distribution).

2.2.2. CaM binding is key to the FMN–heme IET

In the absence of CaM, no IET was observed in the laser flash photolysis experiments for the nNOS and eNOS holoenzymes, showing that CaM is the primary factor in controlling the FMN–heme IET [157, 185]. The formation of the NOS output state involves two primary steps: (i) CaM-binding triggered dissociation of the FMN domain from its reductase binding site, and (ii) subsequent re-association of FMN with the oxygenase domain [158] (Figure 12). Calcium-dependent CaM binding to eNOS/nNOS unlocks the input state, thereby enabling the FMN domain to shuttle between the FAD and heme domains [157, 158]. The NOS state formed at step (i) is competent to reduce cyt *c*, which requires accessibility of FMN to cyt *c*. This is a necessary but not a sufficient condition for NO production by eNOS/nNOS, which in addition requires additional CaM-dependent promotion of the oxygenase/FMN domain interactions. This is strongly supported by the results of a recent study showing that NAPDH reduction is three orders of magnitude faster than NO production, and cyt *c* reduction is intermediate between the two [65].

It is also interesting that the reduction of NOS heme and of cyt *c* both require release of the FMN domain from the input state, but that V_{max} for cyt *c* reduction [116] is an order of magnitude faster than the reduction of NOS heme measured by laser flash photolysis. In cyt *c* reduction reaction, the rate of formation of the complex with cyt *c* is the second order rate constant (for cyt *c* complex formation) times the concentration of NOS molecules with accessible FMN binding domains. The rapid rate of cyt *c* reduction could be accounted by considering the “free” FMN binding domain as partitioning into a range of conformational states. If a much larger number of these states are accessible to cyt *c* than to the NOSoxy domain, one would expect much more rapid reduction of cyt *c* under saturated cyt *c* concentration. This is a reasonable expectation given the small size of cyt *c* and the conformational constraints placed on the oxygenase/FMN complex by the dimeric structure of NOS and the connecting polypeptides linking the domains.

Emerging evidence indicates that CaM is also important for proper alignment of the FMN and heme domains in iNOS [65, 155]. A recent IET kinetics study of a human iNOS oxyFMN protein co-expressed with the N-terminal Ca^{2+}-binding domains of CaM (residues

1–75) indicated that CaM, in particular its N-terminal half, is important in proper alignment of the FMN and heme domains in iNOS [189].

Previously, CaM control of NOS electron transfer was believed to be primarily localized within the reductase portion of the enzyme [190]. Evidence for multiple steps of CaM control was attributed to separate CaM modulation of FMN reduction and heme reduction. The recent experiments have clearly demonstrated CaM dependence outside the reductase complex, *i.e.* CaM-dependent formation of the output state, through the FMN domain interacting with the heme domain [158]. This may be the original role of CaM in the evolution of NOS proteins, and could predate the evolution of the modern control elements.

2.2.3. Role of interdomain interaction in the NOS IET

Biological electron transfer systems depend on proper interactions between proteins/domains that shuttle electron(s) [191–194]. Electrostatic interactions between protein/domain surfaces are important in molecular recognition, making the distribution of charged surface amino acids an active determinant of electron transfer (ET) kinetics [192, 195]. The contacts between the heme and FMN domains of NOS is highly specific because if the FMN domain of nNOS is replaced by its counterpart from the cytochrome P450 reductase, the resultant chimeric enzymes no longer support electron transfer from FMN to heme, despite their similar ET functions [196]. Based on the crystal structures of the functional NOS reductase [40] and oxygenase domains [197], the calculated electrostatic surface potentials reveal a highly positively charged back face of the heme in the oxygenase domain (Figure 14a), and a negatively charged FMN edge (Figure 14b), respectively. These charged residues are conserved in the three NOS isoforms. The plausible FMN-docking site on the oxygenase domain in human eNOS is the back surface near the heme edge containing K175, K192, K429, and K436 (Fig. 14a), where the distance between the heme and protein surface is shortest. This is supported by the mutational studies that implicate a crucial role of residue K423 in rat nNOS, the equivalent residue of K436 in human eNOS, in NO synthesis by nNOS [198]. Mutational studies [199, 200] further indicated that the complementary interdomain FMN/heme and FMN/FAD electrostatic interactions of these sites are critical in the FMN–heme and FMN–FAD IET processes by guiding the interdomain docking. Moreover, pronounced isoform-specific effects of salt concentration on NOS activities have been reported [201]. These results demonstrate that the electrostatic interactions guide the precise docking of the FMN domain to the heme domain (Figure 13).

The comment that the FMN-heme domain interaction is highly specific (see above) may be partially true. ET complexes are a bit different than other types of protein-protein interactions. The ET complexes must form, pass electrons, and then split apart. Some known ET complexes show non-specific inter-protein pairs even though the complexes are dependent on electrostatic interactions; typical examples include: ferredoxin-ferredoxin $NADP^+$ reductase [202], cytochrome *c*-cytochrome *c* peroxidase [203, 204] and cytochrome c2-photosynthetic reaction center [205, 206]. What might be specific in the NOS FMN-heme interactions are complementary electrostatic surfaces but not specific ion pairing. Interestingly, Hoffman lab developed a strategy for redesigning the interface between dynamically docked ET partner proteins, thereby electrostatically strengthening their reactive binding, by optimizing the placement of surface charges within the putative docking interface [207]. This leads to the fastest interprotein ET rate constants yet observed [208].

Besides electrostatic interactions, complementary hydrophobic interactions between aromatic amino acids may also be involved in the FMN-heme interdomain interactions. For example, steady state kinetic studies suggest that Trp421 in the oxygenase domain of nNOS may face towards the reductase domain, playing an important role in the IET [209]. It is likely that changing Trp421 to His may affect the IET kinetics. If so, studies of mutants of

this residue and other hydrophobic surface amino acids shall provide evidence concerning complementary interaction sites between the heme and FMN domains.

2.2.4. Role of the tethers in the NOS IET

There are two tethers for the FMN domain motion in the tethered shuttle model (Figure 12): the hinge region, which is between the FMN and connecting domains (Figure 3), and the CaM binding region between the FMN and oxygenase domains. An important question is how the tethers act in ways to give the FMN domain both an appropriate freedom (to move closer to the heme or FAD domain) while simultaneously providing the necessary restriction to dock precisely. An interesting study showed that the hinge region is important in constraining the activity of eNOS relative to other NOS enzymes [177]. Moreover, the fact that the hinge substitution did not completely convert eNOS to nNOS (in terms of the NO synthesis activity) implies that other structural elements of the eNOS reductase domain must also help restrict electron flux to the heme [177]. These results support a synergistic control mechanism of formation of the NOS output state through CaM binding and intrinsic control elements such as the AR insert and CT.

The NOS reductase domain is homologous to the P450 reductase. Interestingly, a variant of P450 reductase, with a 4-amino acid deletion in the hinge connecting the FMN domain to the rest of the protein, has been crystallized in an open conformation capable of reducing cyt P450, but defective in transferring electrons from FAD to FMN [180]. This study indicates that the hinge regulates the IET processes from FAD to FMN and from FMN to P450 heme by adjusting the distance and orientation of the flavin cofactors [180].

2.2.5. Role of autoregulatory insert in the IET

The unique AR insert within the FMN domain of eNOS and nNOS isoforms is originally identified from sequence alignments and modeling and postulated to restrict alignment of the FMN binding domain with the oxygenase and/or FAD binding domains [66]. Recently, the crystal structure of intact nNOS reductase unit (Figure 3) reveals that, in the absence of CaM, this insert locks the FMN binding domain to the reductase complex via a network of hydrogen bonds so as to obstruct CaM binding and enzyme activation [40]. When CaM binds at high [Ca^{2+}], the insert is believed to be displaced and the enzyme can then be activated. Evidence for a conformational change in this region upon CaM binding came from both proteolysis and fluorescence experiments [66].

Increasing evidence show that the AR insert exerts its regulatory function not only through competing with CaM binding (thus reducing the apparent affinity of the enzyme for CaM) [21], but also through stabilizing certain NOS state via interdomain interactions. The AR-deletion mutant of nNOS in the presence of CaM has only 30 – 50 % NO synthesis activity, indicating disruption of precise FMN/heme interdomain interactions in the mutants [114]. In other words, the AR insert is important for realignment of the FMN and heme domains. Importantly, recent studies by Masters and coworkers suggest that the AR is involved in stabilizing the “open” conformation of the FMN domain for NO synthesis [67]. Indeed, our recent IET kinetics studies on the AR-deletion mutant of nNOS holoenzyme indicate an important role of the AR insert in stabilizing interdomain FMN–heme interactions in the output state, rather than simply playing the role of an inhibitory element [66]. In the crystal structure of the nNOS reductase [40], the AR insert is well positioned to interact with the oxygenase or FMN domain; 28 of the 42 residues in the AR region are not observable (Figure 3), suggesting flexibility of this region. Interestingly, the AR insert is shown to control the conformational equilibrium of the nNOS reductase domain [182]. This was originally proposed by Roman and Masters [67]. These results need to be extended by future dynamic and structural studies in which the conformational space explored by the AR insert

will be elucidated, and to provide insights into how this is changed by CaM binding without sterically blocking the interactions between the FMN and heme domains.

3. Roles of the docked FMN domain in tuning NOS heme structure and activity

The interdomain FMN/heme docking primarily enables the FMN–heme IET (see above). In addition, emerging evidence clearly showed that the docking regulates the NOS catalysis by modulating ferrous heme-NO oxidation reactivity in nNOS [210] and structure [170, 171] of the heme active site in iNOS. Another recent kinetics study also showed that a residue in the FMN domain of iNOS is critical for activity of iNOS [211].

Low temperature MCD spectroscopic studies were conducted to compare the ferric heme centers in wild type (wt) human iNOS oxyFMN and its mutants at the FMN domain (E546N and E603N) [171]; these charged surface residues are conserved in the NOS isoforms, and located at the edge of FMN domain (Figure 5). The low-temperature and VTVH MCD studies by Kirk [171] are the first of their kind on a NOS protein. The low temperature MCD spectra of the wt protein and the mutants are remarkably different [123]: except for the L-Arg-bound wt protein, all other MCD spectra are reminiscent of low-spin ferric heme species [123, 212]. The wt protein possesses a notable change in the Soret region of the MCD spectrum upon addition of L-Arg, whereas the mutant E546N has similar spectra in both the presence and absence of L-Arg [171]. Importantly, the spectroscopic perturbation induced by L-Arg binding in the wt protein is absent in the iNOSoxy construct, where only the heme domain is present [171]; the oxygenase construct thus provides an important control to assess the effects of a properly aligned FMN domain in the wt construct. These results clearly indicate that it is the interactions from the docked FMN domain that contribute to the observed L-Arg-perturbation in the wt protein, and that the conserved residues in the FMN domain are important in productive FMN–heme realignment [171]. This is the first work that provides key evidence for the FMN domain regulating NOS catalytic activity by modulating heme electronic structure *via* the interdomain FMN–heme interactions. Recently, an interesting kinetic study provided further support for the role of the FMN domain in regulating NOS catalytic activity [210]. Here, a neutralization mutation at the nNOS FMN domain surface increases NO synthesis activity by enhancing the rate of ferrous heme–NO oxidation. These kinetic studies thus provide strong support for the model originally proposed by Feng and Kirk in ref. [171].

Moreover, the E→N mutation at E546 in the FMN domain modulates MCD spectra of ferric cyano complexes in a substrate-specific manner [170]. Addition of L-Arg to the wt protein causes notable changes in the CN^--adduct MCD spectrum, while the E546N mutant spectrum is not perturbed (Figure 15). Additionally, the MCD spectroscopic perturbation observed with L-Arg is absent in the CN^- complexes incubated with NOHA, which is the substrate for the second step of NOS catalysis (Scheme 1). EPR spectroscopy also reveals a substrate dependence on the spectra [170]. In light of our recent FMN···heme distance data [163], these results indicate that the interdomain FMN–heme interactions exert a *long-range* effect on key heme axial ligand-substrate interactions (Figure 15). Note that the ferric-cyano complex is a mimic of the obligatory heme-peroxo intermediates of NOS catalysis, and the nature of the axial ligand-substrate interaction in the intermediates is critical in determining the NOS substrate oxidation pathways [18, 20]. Importantly, this combined MCD and EPR spectroscopic work provides key evidence for the FMN domain regulating NOS catalytic activity by modulating heme electronic structure via the interdomain FMN–heme interactions [170].

In the P450cam monooxygenase system, putidaredoxin (Pdx), which transfers electrons to P450cam, can also serve as an effector (recently reviewed in [213]). The binding of Pdx to P450cam induces structural changes in the P450cam active site that couple electron transfer to substrate hydroxylation. It will be interesting to study how the FMN domain docking to the heme domain, in addition to controlling the catalytically essential FMN–heme IET, modulates the reactivity of the heme active site.

4. Perspective

The major outstanding question in NOS catalysis concerns the mechanism by which electron transfer is coupled to substrate oxidation and NO production. Given the large number of variables to deal with, including multiple domain-domain and protein-protein interactions, it is no surprise that this question has not been fully answered yet. It has become clear that our understanding of NOS enzymes will be vertically improved by increasing applications of a combined approach of molecular biology, rapid kinetics (laser flash photolysis and stopped flow), freeze-quench, advanced spectroscopy (including pulsed EPR, low temperature and VTVH MCD, in combination of DFT calculations to relate the experimental parameters to specific active site structures), protein crystallography, and computational modeling. It has been difficult to design selective NOS inhibitors because of the highly conserved active sites of the three human NOS isoforms. An improved understanding of the role of FMN/heme interdomain interaction and calmodulin binding may serve as the basis for the design of new selective inhibitors of NOS isoforms. This is clearly a fertile area for future study. Although considerable progress has been obtained, some outstanding questions remain unanswered, and certainly merit further investigation at the molecular level. These are summarized as follows.

1. Recent kinetics, spectroscopic and crystal structural data help us better understand the role of interdomain interactions in the FMN–heme IET, and raise important mechanistic questions that must be addressed: (i) how do CaM domains specifically interact with NOS isoforms to facilitate the FMN–heme alignment in an isoform-specific manner? (ii) how do intrinsic regulatory elements specifically modulate formation of the output state for NO production in NOS isoforms, and more importantly, how can the modifications of the IET be correlated with the regulatory function of corresponding posttranslational modifications *in vivo*? (iii) is the interdomain FMN/heme alignment responsible for the different IET and NO synthesis activities of the three NOS isoforms? Detailed spectroscopic and kinetics techniques are vital to probe how the interdomain interactions are involved in the IET and NOS catalysis at the molecular level.

2. Because the FMN domain motion is key to the NOS IET processes, there is a clear correlation between the conformational equilibrium and overall NOS activity in the isoforms [96, 214]. The equilibrium between the free and docked FAD/FMN states can be probed by single turn-over stopped flow technique [35, 140]. This conformational equilibrium distinguishes catalysis by the eNOS and nNOS flavoproteins [140]. It is, however, challenging to assess the equilibrium between the free and docked FMN/heme states. Independent determination of the interdomain FMN/heme binding equilibrium is important for interpretation of the EPR and IET data. One potential approach is fluorescence lifetime measurement [188]. This is based on the fact that: (i) the characteristic fluorescence of NOS flavin at 525 nm is a sensitive probe for the local environment of the FMN cofactor [140, 215]; and (ii) the association between the NOS heme and FMN domains can place the FMN molecule close enough to the paramagnetic heme for the FMN fluorescence being quenched [188]. An interesting fluorescence dynamics study indicated that the heme cofactor is involved in formation of the interdomain

interface for conformational changes [216]. Another approach to probe the equilibrium is pulsed EPR techniques. Interestingly, ELDOR has been recently used to study diradical form of P450 reductase, which shed new insight into energy landscapes for the IET mediated by conformational sampling mechanism [217].

3. The knowledge of the docking geometry of the oxygenase and reductase domains, including the distance and orientation between the heme and FMN centers, is desirable for better understanding the FMN–heme IET mechanism. RIDME [163] and pulsed ENDOR [173] have been used to assess the interdomain distance and orientation in the [Fe(III)][FMNH$^{\bullet}$] form of wild type iNOS construct. Four areas related to the interdomain FMN/heme alignment should be further explored. (i) It will be interesting to study other NOS forms/intermediates. In particular, the biopterin radical is a key player in NOS catalysis, and it is important to look at distance between the radical and other cofactors in NOS. Here freeze-quench is needed to trap the intermediates [54, 147]. (ii) Comparative studies of NOS isoforms should be conducted. The IET rate constant of eNOS holoenzyme is nearly ten-fold slower than nNOS and iNOS [185], and an imperfect alignment in eNOS could be responsible for such difference. (iii) Estimation of distance distribution by pulsed EPR should be explored. (iv) It is important to study the alignment as a function of specific residues. The data will be complementary to the kinetics and functional studies of the NOS mutants.

4. Good evidence has been obtained to show that FMN domain docking to the heme domain modulates the reactivity [210] and structure [170, 171] of the heme active site. The key question here is how the docked FMN domain modulates the reactivity of heme active site in an adjacent domain. Our recent MCD and EPR studies indicate that the docked FMN domain affects crucial substrate-axial ligand (e.g. CN^{-}) interactions, and more importantly, this effect is substrate-specific [170]. Note that the NOS cyano adduct is a close mimic to the obligatory heme-dioxygen intermediates. These studies set the stage to further investigate molecular mechanism underlying the FMN domain functions. A promising way to tackle this problem is a combined MCD and EPR approach (Table 1). The low temperature MCD spectra of NOS proteins serve as a site specific probe of perturbations at the heme active site, including proximal Fe–S interactions via the magnitude of the zero-field splitting (ZFS). Additionally, VTVH MCD data can be analyzed using a fit/simulation program [218], to obtain detailed information of ground states of the enzyme active sites. The obtained ZFS parameters (D, E) and g-values can be confirmed by simulation of EPR spectra [219]. It is also of note that ENDOR and ESEEM can probe 1st and 2nd sphere coordination environment of the heme site (type of magnetic nuclei, distance and direction), and thus may provide insight into how the FMN domain docking tunes the heme site structure, particularly of axial ligand (Table 1).

5. The dynamic properties of CaM and the conformational changes that CaM causes in the NOS enzymes make the CaM/NOS complex a very interesting inter-protein interaction model system. Future crystal structural studies toward a CaM-bound full length NOS protein will hopefully clarify how the binding of CaM causes global and local conformational changes in the NOS enzymes to initiate NO synthesis. It is also important to investigate the *dynamic* structural effects of CaM on the NOS enzyme in solution. Two aspects of the CaM-NOS interaction that are of fundamental interest are: how CaM (i) binds, and (ii) activates the three isoforms of NOS.

6. Computational modeling and simulation are certainly required to provide potential rationales and guides for the role of specific amino acids in the IET and NOS

catalysis process. Recently DFT [220–222] and molecular dynamics [223] have been used to study the NOS electron transfer mechanism and substrate oxidation pathways. Interestingly, molecular dynamics have been used to examine active site dynamics and large-scale domain motions of sulfite oxidase [224, 225], in which the interdomain docking is also required for effective IET and catalysis [226–228].

5. Final remarks

Mammalian NOS that comes in three differently regulated isoforms is responsible for generation of NO, a ubiquitous molecule in regulating several physiological functions. The NOS enzyme is tightly regulated to provide NO concentration levels required to carry out normal signaling functions but not to cause deleterious effects. Deviated NO synthesis by NOS is associated with an increasing number of human pathologies. It has been challenging to design selective NOS inhibitors because of the highly conserved active sites of the three human NOS isoforms. Clinical NOS inhibitor remains elusive due to incomplete understanding of molecular mechanism of NOS isoform regulation.

The major outstanding question in NOS regulation concerns the mechanism by which the electron transfer is coupled to substrate oxidation and NO production. Structurally, NOS protein contains FMN and heme domains that are connected by a CaM-binding linker. Compelling evidence clearly demonstrates the importance of the interdomain FMN/heme docking in NOS enzyme regulation (by controlling the physiologically essential FMN–heme IET and modulating reactivity and structure of the heme active site). However, the molecular mechanism by which the FMN domain functions in the NOS catalysis is unclear. An improved understanding of the role of interdomain FMN/heme interaction and CaM binding may serve as the basis for the design of new selective inhibitors of NOS isoforms.

The structure of mammalian NOS holoenzyme has eluded investigators in the field and remains a significant and important challenge. In the absence of a structure of full-length NOS, a combined approach of spectroscopic (e.g. pulsed EPR, MCD, resonance Raman), rapid kinetics and mutagenesis methods is required to unravel the molecular details of the interdomain FMN/heme interactions. This is to investigate the role of the docking between the primary functional FMN and heme domains in regulating NOS activity. We believe that such work will bring in new key insights on how the reactivity at the heme active site is modulated, which is an important and unresolved question in NOS regulation. These studies will also have important mechanistic implications for a large family of related enzymes, including P450 reductase.

Highlights

- Mammalian NOS enzyme is a homodimeric flavo-hemoprotein, and its catalysis is tightly regulated.
- A key question is how interdomain electron transfer is coupled to NO production.
- Absence of a full-length NOS structure justifies a combined spectroscopic and kinetics approach.
- Applications of laser flash photolysis and pulsed EPR to study of NOS FMN-heme complex are reviewed.
- Current understanding of mechanism of electron transfer and interdomain interaction is discussed.

Acknowledgments

We thank many colleagues who have worked with us on NOS enzymes. In particular we are grateful to Prof. Gordon Tollin and Dr. Andrei Astashkin at the University of Arizona, Prof. Martin Kirk at the University of New Mexico, Prof. Guy Guillemette at University of Waterloo, Prof. Bettie Sue Masters and Dr. Linda Roman at the University of Texas Health Science Center at San Antonio, Prof. John Salerno at Kennesaw State University and Dr. Dipak Ghosh at Duke University for critical discussions during our collaborations. We also thank Prof. John Enemark and Prof. F. Ann Walker at the University of Arizona and Prof. Ah-Lim Tsai at the University of Texas Health Science Center at Houston for helpful discussions and encouragements. The research was supported by grants to CF from the National Institutes of Health (GM081811 and HL091280), AHA Grant-in-Aid (09GRNT2220310), and the PhRMA Foundation. The project described was also supported by Grant Number P20RR016480 from the National Center for Research Resources (NCRR), a component of the National Institutes of Health. CF acknowledges the support of UNM HSC RAC grants.

ABBREVIATIONS

NO	nitric oxide
NOS	nitric oxide synthase
iNOS	inducible NOS
nNOS	neuronal NOS
eNOS	endothelial NOS
cNOS	constitutive NOS
NOSoxy	oxygenase domain of NOS
NOSred	reductase domain of NOS
CaM	calmodulin
AR insert	autoregulatory insert within the NOS FMN domain that exists in cNOS, but not in iNOS
oxyFMN	bi-domain NOS construct in which only the oxygenase and FMN domains along with the CaM-binding region are present
FMN	flavin mononucleotide
$FMNH^{\bullet}$	FMN semiquinone
FMN_{hq}	FMN hydroquinone
FAD	flavin adenine dinucleotide
$FADH^{\bullet}$	FAD semiquinone
FAD_{hq}	FAD hydroquinone
AR	cNOS unique autoregulatory insert in the FMN domain
CT	C-terminal tail
cyt	cytochrome
dRF	5-deazariboflavin
L-Arg	L-arginine
NOHA	N-hydroxy-L-arginine
H_4B	(6R)-5,6,7,8-tetrahydrobiopterin
IET	interdomain electron transfer
ET	electron transfer

FNR	ferredoxin-$NADP^+$-reductase
wt	wild type protein
EPR	electron paramagnetic resonance
ENDOR	electron-nuclear double resonance
ESE	electron spin echo
ESEEM	electron spin echo envelope modulation
RIDME	relaxation-induced dipolar modulation enhancement
ELDOR	electron-electron double resonance
MCD	magnetic circular dichroism
VTVH MCD	variable-temperature variable-field MCD

REFERENCES

1. Schmidt H, Walter U. Cell. 1994; 78:919–925. [PubMed: 7923361]
2. Moncada S, Higgs EA. Br J Pharmacol. 2006; 147:S193–S201. [PubMed: 16402104]
3. Montague P, Gancayco C, Winn M, Marchase R, Friedlander M. Science. 1994; 263:973–977. [PubMed: 7508638]
4. Stuehr DJ, Gross SS, Sakuma I, Levi R, Nathan CF. J. Exp. Med. 1989; 169:1011–1020. [PubMed: 2784476]
5. MacMicking J, Xie Q-W, Nathan C. Annu. Rev. Immunol. 1997; 15:323–350. [PubMed: 9143691]
6. Drapier J-C, Pellat C, Henry J. J. Biol. Chem. 1991; 266:10162–10167. [PubMed: 1645341]
7. Stadler J, Bergonia HA, Di Silvio M, Sweetland MA, Billiar TR, Simmons R, Lancaster JR. Arch. Biochem. Biophys. 1993; 302:4–11. [PubMed: 8385904]
8. Terenzi F, Diaz-Guerra JM, Casado M, Hortelano S, Leoni S, Boscá L. J. Biol. Chem. 1995; 270:6017–6021. [PubMed: 7534305]
9. Lundberg JO, Carlström M, Larsen FJ, Weitzberg E. Cardiovasc Res. 2011; 89:525–532. [PubMed: 20937740]
10. Zuckerbraun BS, George P, Gladwin MT. Cardiovasc Res. 2011; 89:542–552. [PubMed: 21177703]
11. Lancaster JR, Xie KP. Cancer Res. 2006; 66:6459–6462. [PubMed: 16818612]
12. Vallance P, Leiper J. Nature Reviews Drug Discovery. 2002; 1:939–950.
13. Delker SL, Ji H, Li H, Jamal J, Fang J, Xue F, Silverman RB, Poulos TL. J. Am. Chem. Soc. 2010; 132:5437–5442. [PubMed: 20337441]
14. Alderton WK, Cooper CE, Knowles RG. Biochem. J. 2001; 357:593–615. [PubMed: 11463332]
15. Zhu Y, Silverman RB. Biochemistry. 2008; 47:2231–2243. [PubMed: 18237198]
16. Santolini J. J. Inorg. Biochem. 2011; 105:127–141. [PubMed: 21194610]
17. Daff S. Nitric Oxide. 2010; 23:1–11. [PubMed: 20303412]
18. Davydov R, Sudhamsu J, Lees NS, Crane BR, Hoffman BM. J. Am. Chem. Soc. 2009; 131:14493–14507. [PubMed: 19754116]
19. Woodward JJ, NejatyJahromy Y, Britt RD, Marletta MA. J. Am. Chem. Soc. 2010; 132:5105–5113. [PubMed: 20307068]
20. Li D, Kabir M, Stuehr DJ, Rousseau DL, Yeh SR. J. Am. Chem. Soc. 2007; 129:6943–6951. [PubMed: 17488012]
21. Roman LJ, Martasek P, Masters BSS. Chem. Rev. 2002; 102:1179–1189. [PubMed: 11942792]
22. Bredt DS, Hwang PM, Glatt CE, Lowenstein C, Reed RR, Snyder SH. Nature. 1991; 351:714–718. [PubMed: 1712077]

23. Murataliev MB, Feyereisen R, Walker FA. Biochimica et Biophysica Acta (BBA) - Proteins & Proteomics. 2004; 1698:1–26.
24. Wang M, Roberts DL, Paschke R, Shea TM, Masters BSS, Kim JJP. Proc Natl Acad Sci U S A. 1997; 94:8411–8416. [PubMed: 9237990]
25. Stevenstruss R, Marletta MA. Biochemistry. 1995; 34:15638–15645. [PubMed: 7495792]
26. Baek KJ, Thiel BA, Lucas S, Stuehr DJ. J. Biol. Chem. 1993; 268:21120–21129. [PubMed: 7691806]
27. Crane BR, Arvai AS, Gachhui R, Wu CQ, Ghosh DK, Getzoff ED, Stuehr DJ, Tainer JA. Science. 1997; 278:425–431. [PubMed: 9334294]
28. Albakri QA, Stuehr DJ. J. Biol. Chem. 1996; 271:5414–5421. [PubMed: 8621396]
29. Raman CS, Li HY, Martasek P, Kral V, Masters BSS, Poulos TL. Cell. 1998; 95:939–950. [PubMed: 9875848]
30. Ghosh DK, Abu-Soud HM, Stuehr DJ. Biochemistry. 1996; 35:1444–1449. [PubMed: 8634274]
31. Panda K, Ghosh S, Stuehr DJ. J. Biol. Chem. 2001; 276:23349–23356. [PubMed: 11325964]
32. Ghosh DK, Abu-soud HM, Stuehr DJ. Biochemistry. 1995; 34:11316–11320. [PubMed: 7547858]
33. Roman LJ, Sheta EA, Martasek P, Gross SS, Liu Q, Masters BSS. Proc Natl Acad Sci U S A. 1995; 92:8428–8432. [PubMed: 7545302]
34. Sheta EA, McMillan K, Masters BSS. J. Biol. Chem. 1994; 269:15147–15153. [PubMed: 7515050]
35. Ilagan RP, Tejero JS, Aulak KS, Ray SS, Hemann C, Wang Z-Q, Gangoda M, Zweier JL, Stuehr DJ. Biochemistry. 2009; 48:3864–3876. [PubMed: 19290671]
36. Ghosh DK, Holliday MA, Thomas C, Weinberg JB, Smith SME, Salerno JC. J. Biol. Chem. 2006; 281:14173–14183. [PubMed: 16461329]
37. Crane BR, Arvai AS, Ghosh DK, Wu CQ, Getzoff ED, Stuehr DJ, Tainer JA. Science. 1998; 279:2121–2126. [PubMed: 9516116]
38. Li HY, Shimizu H, Flinspach M, Jamal J, Yang WP, Xian M, Cai TW, Wen EZ, Jia QA, Wang PG, Poulos TL. Biochemistry. 2002; 41:13868–13875. [PubMed: 12437343]
39. Zhang J, Martasek P, Paschke R, Shea T, Masters BSS, Kim JJP. J. Biol. Chem. 2001; 276:37506–37513. [PubMed: 11473123]
40. Garcin ED, Bruns CM, Lloyd SJ, Hosfield DJ, Tiso M, Gachhui R, Stuehr DJ, Tainer JA, Getzoff ED. J. Biol. Chem. 2004; 279:37918–37927. [PubMed: 15208315]
41. Xia C, Misra I, Iyanagi T, Kim J-JP. J. Biol. Chem. 2009; 284:30708–30717. [PubMed: 19737939]
42. Aoyagi M, Arvai AS, Tainer JA, Getzoff ED. EMBO J. 2003; 22:766–775. [PubMed: 12574113]
43. Doukov T, Li H, Sharma A, Martell JD, Soltis SM, Silverman RB, Poulos TL. J. Am. Chem. Soc. 2011; 133:8326–8334. [PubMed: 21534614]
44. Martell JD, Li H, Doukov T, Martásek P, Roman LJ, Soltis M, Poulos TL, Silverman RB. J. Am. Chem. Soc. 2009; 132:798–806. [PubMed: 20014790]
45. Garcin ED, Arvai AS, Rosenfeld RJ, Kroeger MD, Crane BR, Andersson G, Andrews G, Hamley PJ, Mallinder PR, Nicholls DJ, St-Gallay SA, Tinker AC, Gensmantel NP, Mete A, Cheshire DR, Connolly S, Stuehr DJ, Aberg A, Wallace AV, Tainer JA, Getzoff ED. Nat Chem Biol. 2008; 4:700–707. [PubMed: 18849972]
46. Fedorov R, Vasan R, Ghosh DK, Schlichting I. Proc Natl Acad Sci U S A. 2004; 101:5892–5897. [PubMed: 15071192]
47. Konas DW, Takaya N, Sharma M, Stuehr DJ. Biochemistry. 2006; 45:12596–12609. [PubMed: 17029414]
48. Tiso M, Konas DW, Panda K, Garcin ED, Sharma M, Getzoff ED, Stuehr DJ. J. Biol. Chem. 2005; 280:39208–39219. [PubMed: 16150731]
49. Panda K, Adak S, Konas D, Sharma M, Stuehr DJ. J. Biol. Chem. 2004; 279:18323–18333. [PubMed: 14966111]
50. Konas DW, Zhu K, Sharma M, Aulak KS, Brudvig GW, Stuehr DJ. J. Biol. Chem. 2004; 279:35412–35425. [PubMed: 15180983]
51. Wang ZQ, Wei CC, Stuehr DJ. J. Biol. Chem. 2002; 277:12830–12837. [PubMed: 11823464]

52. Poulos TL. Drug Metab Dispos. 2005; 33:10–18. [PubMed: 15475411]
53. Raman CS, Li HY, Martasek P, Southan G, Masters BSS, Poulos TL. Biochemistry. 2001; 40:13448–13455. [PubMed: 11695891]
54. Stoll S, NejatyJahromy Y, Woodward JJ, Ozarowski A, Marletta MA, Britt RD. J. Am. Chem. Soc. 2010; 132:11812–11823. [PubMed: 20669954]
55. Chen W, Druhan LJ, Chen C-A, Hemann C, Chen Y-R, Berka V, Tsai A-L, Zweier JL. Biochemistry. 2010
56. Rosen GM, Tsai P, Weaver J, Porasuphatana S, Roman LJ, Starkov AA, Fiskum G, Pou S. J. Biol. Chem. 2002; 277:40275–40280. [PubMed: 12183447]
57. Vasquez-Vivar J, Kalyanaraman B, Martasek P, Hogg N, Masters BSS, Karoui H, Tordo P, Pritchard KA. Proc Natl Acad Sci U S A. 1998; 95:9220–9225. [PubMed: 9689061]
58. Hurshman AR, Krebs C, Edmondson DE, Huynh BH, Marletta MA. Biochemistry. 1999; 38:15689–15696. [PubMed: 10625434]
59. Xue F, Li H, Fang J, Roman LJ, Martásek P, Poulos TL, Silverman RB. Bioorg. Med. Chem. Lett. 2010; 20:6258–6261. [PubMed: 20833542]
60. Doukov T, Li HY, Soltis M, Poulos TL. Biochemistry. 2009; 48:10246–10254. [PubMed: 19791770]
61. Knudsen GM, Nishida CR, Mooney SD, de Montellano PRO. J. Biol. Chem. 2003; 278:31814–31824. [PubMed: 12805387]
62. Gachhui R, Abu-Soud HM, Ghosh DK, Presta A, Blazing MA, Mayer B, George SE, Stuehr DJ. J. Biol. Chem. 1998; 273:5451–5454. [PubMed: 9488666]
63. George SE, Su ZH, Fan DJ, Means AR. J. Biol. Chem. 1993; 268:25213–25220. [PubMed: 8227086]
64. Greif DM, Sacks DB, Michel T. Proc Natl Acad Sci U S A. 2004; 101:1165–1170. [PubMed: 14736917]
65. Newman E, Spratt DE, Mosher J, Cheyne B, Montgomery HJ, Wilson DL, Weinberg JB, Smith SME, Salerno JC, Ghosh DK, Guillemette JG. J. Biol. Chem. 2004; 279:33547–33557. [PubMed: 15138276]
66. Salerno JC, Harris DE, Irizarry K, Patel B, Morales AJ, Smith SME, Martasek P, Roman LJ, Masters BSS, Jones CL, Weissman BA, Lane P, Liu Q, Gross SS. J. Biol. Chem. 1997; 272:29769–29777. [PubMed: 9368047]
67. Roman LJ, Masters BSS. J. Biol. Chem. 2006; 281:23111–23118. [PubMed: 16782703]
68. Tejero J, Haque MM, Durra D, Stuehr DJ. J. Biol. Chem. 2010; 285:25941–25949. [PubMed: 20529840]
69. Masters BS, Roman LJ, Martasek P, Feng CJ. Nitric Oxide. 2010; 22:S11.
70. Su ZZ, Blazing MA, Fan D, George SE. J. Biol. Chem. 1995; 270:29117–29122. [PubMed: 7493936]
71. Stevens-Truss R, Marletta MA. FASEB J. 1999; 13:A1531–A1531.
72. Spratt DE, Newman E, Mosher J, Ghosh DK, Salerno JC, Guillemette JG. FEBS J. 2006; 273:1759–1771. [PubMed: 16623711]
73. Tran Q-K, Leonard J, Black DJ, Persechini A. Biochemistry. 2008; 47:7557–7566. [PubMed: 18558722]
74. Tran QK, Leonard J, Black DJ, Nadeau OW, Boulatnikov IG, Persechini A. J. Biol. Chem. 2009; 284:11892–11899. [PubMed: 19251696]
75. Spratt DE, Taiakina V, Palmer M, Guillemette JG. Biochemistry. 2007; 46:8288–8300. [PubMed: 17580957]
76. Spratt DE, Taiakina V, Palmer M, Guillemette JG. Biochemistry. 2008; 47:12006–12017. [PubMed: 18947187]
77. Persechini A, McMillan K, Leakey P. J. Biol. Chem. 1994; 269:16148–16154. [PubMed: 7515878]
78. McMillan K, Bredt DS, Hirsch DJ, Snyder SH, Clark JE, Masters BSS. Proc Natl Acad Sci U S A. 1992; 89:11141–11145. [PubMed: 1280819]
79. White KA, Marletta MA. Biochemistry. 1992; 31:6627–6631. [PubMed: 1379068]

80. Gerber NC, de Montellano PRO. J. Biol. Chem. 1995; 270:17791–17796. [PubMed: 7543092]
81. Martasek P, Liu Q, Liu JW, Roman LJ, Gross SS, Sessa WC, Masters BSS. Biochem. Biophys. Res. Commun. 1996; 219:359–365. [PubMed: 8604992]
82. Ghosh DK, Wu CQ, Pitters E, Moloney M, Werner ER, Mayer B, Stuehr DJ. Biochemistry. 1997; 36:10609–10619. [PubMed: 9271491]
83. Vasquez-Vivar J, Hogg N, Martasek P, Karoui H, Pritchard KA, Kalyanaraman B. J. Biol. Chem. 1999; 274:26736–26742. [PubMed: 10480877]
84. Santolini J, Adak S, Curran CML, Stuehr DJ. J. Biol. Chem. 2001; 276:1233–1243. [PubMed: 11038356]
85. Salerno JC. FEBS Lett. 2008; 582:1395–1399. [PubMed: 18396171]
86. Craig DH, Chapman SK, Daff S. J. Biol. Chem. 2002; 277:33987–33994. [PubMed: 12089147]
87. Adak S, Bilwes AM, Panda K, Hosfield D, Aulak KS, McDonald JF, Tainer JA, Getzoff ED, Crane BR, Stuehr DJ. Proc Natl Acad Sci U S A. 2002; 99:107–112. [PubMed: 11756668]
88. Pant K, Bilwes AM, Adak S, Stuehr DJ, Crane BR. Biochemistry. 2002; 41:11071–11079. [PubMed: 12220171]
89. Crane BR, Sudhamsu J, Patel BA. Annu. Rev. Biochem. 2010; 79:445–470. [PubMed: 20370423]
90. Wang ZQ, Lawson RJ, Buddha MR, Wei CC, Crane BR, Munro AW, Stuehr DJ. J. Biol. Chem. 2007; 282:2196–2202. [PubMed: 17127770]
91. Agapie T, Suseno S, Woodward JJ, Stoll S, Britt RD, Marletta MA. Proceedings of the National Academy of Sciences. 2009; 106:16221–16226.
92. Hannibal L, Somasundaram R, Tejero J, Wilson A, Stuehr DJ. J. Biol. Chem. 2011 in press.
93. Sudhamsu J, Crane BR. J. Biol. Chem. 2006; 281:9623–9632. [PubMed: 16407211]
94. Santolini M, Roman M, Stuehr DJ, Mattioli TA. Biochemistry. 2006; 45:1480–1489. [PubMed: 16445290]
95. Chartier FJM, Couture M. J. Biol. Chem. 2007; 282:20877–20886. [PubMed: 17537725]
96. Stuehr DJ, Tejero J, Haque MM. FEBS J. 2009; 276:3959–3974. [PubMed: 19583767]
97. Stuehr DJ, Santolini J, Wang ZQ, Wei CC, Adak S. J. Biol. Chem. 2004; 279:36167–36170. [PubMed: 15133020]
98. Masters BSS. J. Biol. Chem. 2009; 284:19765–19780. [PubMed: 19398561]
99. Wei CC, Crane BR, Stuehr DJ. Chem. Rev. 2003; 103:2365–2383. [PubMed: 12797834]
100. Feng CJ, Tollin G. Dalton Trans. 2009:6692–6700. [PubMed: 19690675]
101. Xia Y, Roman LJ, Masters BSS, Zweier JL. J. Biol. Chem. 1998; 273:22635–22639. [PubMed: 9712892]
102. Chen CA, Druhan LJ, Varadharaj S, Chen YR, Zweier JL. J. Biol. Chem. 2008; 283:27038–27047. [PubMed: 18622039]
103. Stuehr DJ, Ikeda-Saito M. J. Biol. Chem. 1992; 267:20547–20550. [PubMed: 1383204]
104. Tsai AL, Berka V, Chen PF, Palmer G. J. Biol. Chem. 1996; 271:32563–32571. [PubMed: 8955082]
105. Galli C, MacArthur R, Abu-Soud HM, Clark P, Stuehr DJ, Brudvig GW. Biochemistry. 1996; 35:2804–2810. [PubMed: 8611587]
106. Gao YT, Smith SME, Weinberg JB, Montgomery HJ, Newman E, Guillemette JG, Ghosh DK, Roman LJ, Martasek P, Salerno JC. J. Biol. Chem. 2004; 279:18759–18766. [PubMed: 14715665]
107. Matsuda H, Iyanagi T. Biochimica Et Biophysica Acta-General Subjects. 1999; 1473:345–355.
108. Knight K, Scrutton NS. Biochem. J. 2002; 367:19–30. [PubMed: 12079493]
109. Abusoud HM, Stuehr DJ. Proc. Natl. Acad. Sci. U. S. A. 1993; 90:10769–10772. [PubMed: 7504282]
110. Abusoud HM, Yoho LL, Stuehr DJ. J. Biol. Chem. 1994; 269:32047–32050. [PubMed: 7528206]
111. Noble MA, Munro AW, Rivers SL, Robledo L, Daff SN, Yellowlees LJ, Shimizu T, Sagami I, Guillemette JG, Chapman SK. Biochemistry. 1999; 38:16413–16418. [PubMed: 10600101]
112. Daff S, Noble MA, Craig DH, Rivers SL, Chapman SK, Munro AW, Fujiwara S, Rozhkova E, Sagami I, Shimizu T. Biochem. Soc. Trans. 2001; 29:147–152. [PubMed: 11356143]

113. Dunford AJ, Rigby SEJ, Hay S, Munro AW, Scrutton NS. Biochemistry. 2007; 46:5018–5029. [PubMed: 17411075]
114. Daff S, Sagami I, Shimizu T. J. Biol. Chem. 1999; 274:30589–30595. [PubMed: 10521442]
115. Roman LJ, Miller RT, de la Garza MA, Kim JJP, Masters BSS. J. Biol. Chem. 2000; 275:21914–21919. [PubMed: 10781602]
116. Roman LJ, Martasek P, Miller RT, Harris DE, de la Garza MA, Shea TM, Kim JJP, Masters BSS. J. Biol. Chem. 2000; 275:29225–29232. [PubMed: 10871625]
117. Montgomery HJ, Romanov V, Guillemette JG. J. Biol. Chem. 2000; 275:5052–5058. [PubMed: 10671547]
118. Nishida CR, de Montellano PRO. J. Biol. Chem. 2001; 276:20116–20124. [PubMed: 11264292]
119. Lane P, Gross SS. J. Biol. Chem. 2002; 277:19087–19094. [PubMed: 11839759]
120. Chen PF, Wu KK. J. Biol. Chem. 2000; 275:13155–13163. [PubMed: 10777622]
121. McCabe TJ, Fulton D, Roman LJ, Sessa WC. J. Biol. Chem. 2000; 275:6123–6128. [PubMed: 10692402]
122. Sono M, Stuehr DJ, Ikedasaito M, Dawson JH. J. Biol. Chem. 1995; 270:19943–19948. [PubMed: 7544348]
123. Berka V, Palmer G, Chen P-F, Tsai A-L. Biochemistry. 1998; 37:6136–6144. [PubMed: 9558353]
124. Ledbetter AP, McMillan K, Roman LJ, Masters BSS, Dawson JH, Sono M. Biochemistry. 1999; 38:8014–8021. [PubMed: 10387045]
125. Wang JL, Stuehr DJ, Ikedasaito M, Rousseau DL. J. Biol. Chem. 1993; 268:22255–22258. [PubMed: 7693663]
126. Zhang M, Yuan T, Aramini JM, Vogel HJ. J. Biol. Chem. 1995; 270:20901–20907. [PubMed: 7545663]
127. Cosper NJ, Scott RA, Hori H, Nishino T, Iwasaki T. J. Biochem. 2001; 130:191–198. [PubMed: 11481035]
128. Tierney DL, Martasek P, Doan PE, Masters BSS, Hoffman BM. J. Am. Chem. Soc. 1998; 120:2983–2984.
129. Rousseau DL, Li D, Couture M, Yeh SR. J. Inorg. Biochem. 2005; 99:306–323. [PubMed: 15598509]
130. Hoffman BM. Proc Natl Acad Sci U S A. 2003; 100:3575–3578. [PubMed: 12642664]
131. Ost TWB, Daff S. J. Biol. Chem. 2005; 280:965–973. [PubMed: 15507439]
132. Udit AK, Belliston-Bittner W, Glazer EC, Le Nguyen YH, Gillan JM, Hill MG, Marletta MA, Goodin DB, Gray HB. J. Am. Chem. Soc. 2005; 127:11212–11213. [PubMed: 16089428]
133. Leslie Dutton, P. [23] Redox potentiometry: Determination of midpoint potentials of oxidation-reduction components of biological electron-transfer systems. In: Sidney, F.; Lester, P., editors. Methods Enzymol. Academic Press; 1978. p. 411-435.
134. Hoke KR, Crane BR. Nitric Oxide. 2009; 20:79–87. [PubMed: 19059356]
135. Presta A, Weber-Main AM, Stankovich MT, Stuehr DJ. J. Am. Chem. Soc. 1998; 120:9460–9465.
136. Presta A, Weber-Main AM, Stankovich MT, Stuehr DJ. J. Am. Chem. Soc. 1998; 120:9460–9465.
137. Sanae R, Kurokawa F, Oda M, Ishijima S, Sagami I. Biochemistry. 2011; 50:1714–1722. [PubMed: 21244098]
138. Martasek, P.; Miller, RT.; Roman, LJ.; Shea, T.; Masters, BSS.; Lester, P. Methods Enzymol. Academic Press; 1999. Assay of isoforms of Escherichia coli-expressed nitric oxide synthase; p. 70-78.
139. Guan ZW, Kamatani D, Kimura S, Iyanagi T. J. Biol. Chem. 2003; 278:30859–30868. [PubMed: 12777376]
140. Ilagan RP, Tiso M, Konas DW, Hemann C, Durra D, Hille R, Stuehr DJ. J. Biol. Chem. 2008; 283:19603–19615. [PubMed: 18487202]

141. Abu-Soud HM, Feldman PL, Clark P, Stuehr DJ. J. Biol. Chem. 1994; 269:32318–32326. [PubMed: 7528212]
142. Miller RT, Martasek P, Omura T, Masters BSS. Biochem. Biophys. Res. Commun. 1999; 265:184–188. [PubMed: 10548511]
143. Wei, CC.; Wang, ZQ.; Stuehr, DJ. Enzyme Kinetics and Mechanism, Pt F: Detection and Characterization of Enzyme Reaction Intermediates. San Diego: Academic Press Inc; 2002. Nitric oxide synthase: Use of stopped-flow spectroscopy and rapid-quench methods in single-turnover conditions to examine formation and reactions of heme-O-2 intermediate in early catalysis; p. 320-338.
144. Gorren, ACF.; Sørlie, M.; Andersson, KK.; Marchal, S.; Lange, R.; Mayer, B. Tetrahydrobiopterin as Combined Electron/Proton Donor in Nitric Oxide Biosynthesis: Cryogenic UV-Vis and EPR Detection of Reaction Intermediates. In: Lester, P.; Enrique, C., editors. Methods Enzymol. Academic Press; 2005. p. 456-466.
145. Wei C-C, Wang Z-Q, Tejero J, Yang Y-P, Hemann C, Hille R, Stuehr DJ. J. Biol. Chem. 2008:11734–11742. [PubMed: 18283102]
146. Stuehr DJ, Wei CC, Wang ZQ, Hille R. Dalton Trans. 2005:3427–3435. [PubMed: 16234921]
147. Berka V, Wang LH, Tsai AL. Biochemistry. 2008; 47:405–420. [PubMed: 18052254]
148. Scheele JS, Bruner E, Kharitonov VG, Martasek P, Roman LJ, Masters BSS, Sharma VS, Magde D. J. Biol. Chem. 1999; 274:13105–13110. [PubMed: 10224063]
149. Scheele JS, Kharitonov VG, Martasek P, Roman LJ, Sharma VS, Masters BSS, Magde D. J. Biol. Chem. 1997; 272:12523–12528. [PubMed: 9139703]
150. Stevenson TH, Gutierrez AF, Alderton WK, Lian LY, Scrutton NS. Biochem. J. 2001; 358:201–208. [PubMed: 11485568]
151. Feng C, Fan W, Ghosh DK, Tollin G. Biochimica et Biophysica Acta (BBA) - Proteins & Proteomics. 2011; 1814:405–408.
152. Belliston-Bittner W, Dunn AR, Nguyen YHL, Stuehr DJ, Winkler JR, Gray HB. J. Am. Chem. Soc. 2005; 127:15907–15915. [PubMed: 16277534]
153. Beaumont E, Lambry JC, Gautier C, Robin AC, Gmouh S, Berka V, Tsai AL, Blanchard-Desce M, Slama-Schwok A. J. Am. Chem. Soc. 2007; 129:2178–2186. [PubMed: 17263536]
154. Beaumont E, Lambry JC, Blanchard-Desce M, Martasek P, Panda SP, Faassen EEH, Brochon JC, Deprez E, Slama-Schwok A. Chembiochem. 2009; 10:690–701. [PubMed: 19222033]
155. Feng CJ, Dupont A, Nahm N, Spratt D, Hazzard JT, Weinberg J, Guillemette J, Tollin G, Ghosh DK. J. Biol. Inorg. Chem. 2009; 14:133–142. [PubMed: 18830722]
156. Feng CJ, Roman LJ, Hazzard JT, Ghosh DK, Tollin G, Masters BSS. FEBS Lett. 2008; 582:2768–2772. [PubMed: 18625229]
157. Feng CJ, Tollin G, Hazzard JT, Nahm NJ, Guillemette JG, Salerno JC, Ghosh DK. J. Am. Chem. Soc. 2007; 129:5621–5629. [PubMed: 17425311]
158. Feng CJ, Tollin G, Holliday MA, Thomas C, Salerno JC, Enemark JH, Ghosh DK. Biochemistry. 2006; 45:6354–6362. [PubMed: 16700546]
159. Feng CJ, Thomas C, Holliday MA, Tollin G, Salerno JC, Ghosh DK, Enemark JH. J. Am. Chem. Soc. 2006; 128:3808–3811. [PubMed: 16536556]
160. Tierney DL, Huang H, Martasek P, Roman LJ, Silverman RB, Masters BSS, Hoffman BM. J. Am. Chem. Soc. 2000; 122:5405–5406.
161. Tierney DL, Huang H, Martasek P, Roman LJ, Silverman RB, Hoffman BM. J. Am. Chem. Soc. 2000; 122:7869–7875.
162. Davydov R, Ledbetter-Rogers A, Martasek P, Larukhin M, Sono M, Dawson JH, Masters BSS, Hoffman BM. Biochemistry. 2002; 41:10375–10381. [PubMed: 12173923]
163. Astashkin AV, Elmore BO, Fan W, Guillemette JG, Feng C. J. Am. Chem. Soc. 2010; 132:12059–12067. [PubMed: 20695464]
164. Chen C-A, Wang T-Y, Varadharaj S, Reyes LA, Hemann C, Talukder MAH, Chen Y-R, Druhan LJ, Zweier JL. Nature. 2010; 468:1115–1118. [PubMed: 21179168]
165. Page CC, Moser CC, Chen XX, Dutton PL. Nature. 1999; 402:47–52. [PubMed: 10573417]

166. Lyubenova S, Maly T, Zwicker K, Brandt U, Ludwig B, Prisner T. Acc Chem Res. 2010; 43:181–189. [PubMed: 19842617]
167. Roessler MM, King MS, Robinson AJ, Armstrong FA, Harmer J, Hirst J. Proc Natl Acad Sci U S A. 2010; 107:1930–1935. [PubMed: 20133838]
168. Schiemann O, Prisner TF. Q Rev Biophys. 2007; 40:1–53. [PubMed: 17565764]
169. Codd R, Astashkin AV, Pacheco A, Raitsimring AM, Enemark JH. J. Biol. Inorg. Chem. 2002; 7:338–350. [PubMed: 11935358]
170. Sempombe J, Galinato MGI, Elmore BO, Fan W, Guillemette JG, Lehnert N, Kirk ML, Feng C. Inorg. Chem. 2011; 50:6859–6861. [PubMed: 21718007]
171. Sempombe J, Elmore BO, Sun X, Dupont A, Ghosh DK, Guillemette JG, Kirk ML, Feng C. J. Am. Chem. Soc. 2009; 131:6940–6941. [PubMed: 19405537]
172. Kulik LV, Dzuba SA, Grigoryev IA, Tsvetkov YD. Chem. Phys. Lett. 2001; 343:315–324.
173. Astashkin AV, Fan W, Elmore BO, Guillemette JG, Feng C. The Journal of Physical Chemistry A. 2011; 115:10345–10352. [PubMed: 21834532]
174. Ghosh DK, Salerno JC. Front Biosci. 2003; 8:D193–D209. [PubMed: 12456347]
175. Li H, Das A, Sibhatu H, Jamal J, Sligar SG, Poulos TL. J. Biol. Chem. 2008; 283:34762–34772. [PubMed: 18852262]
176. Welland A, Garnaud PE, Kitamura M, Miles CS, Daff S. Biochemistry. 2008; 47:9771–9780. [PubMed: 18717591]
177. Haque MM, Panda K, Tejero J, Aulak KS, Fadlalla MA, Mustovich AT, Stuehr DJ. Proc Natl Acad Sci U S A. 2007; 104:9254–9259. [PubMed: 17517617]
178. Hubbard PA, Shen AL, Paschke R, Kasper CB, Kim J-JP. J. Biol. Chem. 2001; 276:29163–29170. [PubMed: 11371558]
179. Sevrioukova IF, Li H, Zhang H, Peterson JA, Poulos TL. Proc Natl Acad Sci U S A. 1999; 96:1863–1868. [PubMed: 10051560]
180. Hamdane D, Xia C, Im S-C, Zhang H, Kim J-JP, Waskell L. J. Biol. Chem. 2009; 284:11374–11384. [PubMed: 19171935]
181. Xia C, Hamdane D, Shen AL, Choi V, Kasper CB, Pearl M, Zhang H, Im S-C, Waskell L, Kim J-JP. J. Biol. Chem. 2011; 286:16246–16260. [PubMed: 21345800]
182. Guan Z-W, Haque MM, Wei C-C, Garcin ED, Getzoff ED, Stuehr DJ. J. Biol. Chem. 2010; 285:3064–3075. [PubMed: 19948738]
183. Li HY, Igarashi J, Jamal J, Yang WP, Poulos TL. J. Biol. Inorg. Chem. 2006; 11:753–768. [PubMed: 16804678]
184. Sevrioukova IF, Hazzard JT, Tollin G, Poulos TL. J. Biol. Chem. 1999; 274:36097–36106. [PubMed: 10593892]
185. Feng C, Taiakina V, Ghosh DK, Guillemette JG, Tollin G. Biochimica et Biophysica Acta (BBA) - Proteins & Proteomics. 2011 in press.
186. Li W, Fan W, Elmore BO, Feng C. FEBS Lett. 2011; 585:2622–2626. [PubMed: 21803041]
187. Wu G, Berka V, Tsai A-L. J. Inorg. Biochem. 2011; 105:1226–1237. [PubMed: 21763233]
188. Salerno JC, Ghosh DK, Ray K, Adrados M, Nahm N, Li H, Poulos TI, Lakowicz J. Nitric Oxide. 2010; 22:S12–S12.
189. Feng C, Fan W, Dupont A, Guy Guillemette J, Ghosh DK, Tollin G. FEBS Lett. 2010; 584:4335–4338. [PubMed: 20868689]
190. Gachhui R, Presta A, Bentley DF, Abu-Soud HM, McArthur R, Brudvig G, Ghosh DK, Stuehr DJ. J. Biol. Chem. 1996; 271:20594–20602. [PubMed: 8702805]
191. Hoffman BM, Celis LM, Cull DA, Patel AD, Seifert JL, Wheeler KE, Wang JY, Yao J, Kurnikov IV, Nocek JM. Proc Natl Acad Sci U S A. 2005; 102:3564–3569. [PubMed: 15738411]
192. Tollin G. Electron Transfer in Chemistry. 2001; IV:202–231.
193. Leys D, Scrutton NS. Curr Opin Struct Biol. 2004; 14:642–647. [PubMed: 15582386]
194. Feng CJ, Wilson HL, Hurley JK, Hazzard JT, Tollin G, Rajagopalan KV, Enemark JH. Biochemistry. 2003; 42:12235–12242. [PubMed: 14567685]

195. Hurley JK, Morales R, Martinez-Julvez M, Brodie TB, Medina M, Gomez-Moreno C, Tollin G. Biochimica Et Biophysica Acta-Bioenergetics. 2002; 1554:5–21.
196. Roman LJ, McLain J, Masters BSS. J. Biol. Chem. 2003; 278:25700–25707. [PubMed: 12730215]
197. Fischmann TO, Hruza A, Niu XD, Fossetta JD, Lunn CA, Dolphin E, Prongay AJ, Reichert P, Lundell DJ, Narula SK, Weber PC. Nat Struct Biol. 1999; 6:233–242. [PubMed: 10074942]
198. Shimanuki T, Sato H, Daff S, Sagami I, Shimizu T. J. Biol. Chem. 1999; 274:26956–26961. [PubMed: 10480907]
199. Tejero J, Hannibal L, Mustovich A, Stuehr DJ. J. Biol. Chem. 2010; 285:27232–27240. [PubMed: 20592038]
200. Panda K, Haque MM, Garcin-Hosfield ED, Durra D, Getzoff ED, Stuehr DJ. J. Biol. Chem. 2006; 281:36819–36827. [PubMed: 17001078]
201. Schrammel A, Gorren ACF, Stuehr DJ, Schmidt K, Mayer B. Biochimica Et Biophysica Acta-Protein Structure and Molecular Enzymology. 1998; 1387:257–263.
202. Serre L, Vellieux FMD, Medina M, Gomez-Moreno C, Fontecilla-Camps JC, Frey M. J. Mol. Biol. 1996; 263:20–39. [PubMed: 8890910]
203. Guo M, Bhaskar B, Li H, Barrows TP, Poulos TL. Proc Natl Acad Sci U S A. 2004; 101:5940–5945. [PubMed: 15071191]
204. Kang SA, Crane BR. Proc Natl Acad Sci U S A. 2005; 102:15465–15470. [PubMed: 16227441]
205. Adir N, Axelrod HL, Beroza P, Isaacson RA, Rongey SH, Okamura MY, Feher G. Biochemistry. 1996; 35:2535–2547. [PubMed: 8611557]
206. Abresch EC, Paddock ML, Villalobos M, Chang C, Okamura MY. Biochemistry. 2008; 47:13318–13325. [PubMed: 19053264]
207. Nocek JM, Knutson AK, Xiong P, Petlakh Co N, Hoffman BM. J. Am. Chem. Soc. 2010; 132:6165–6175. [PubMed: 20392066]
208. Xiong P, Nocek JM, Vura-Weis J, Lockard JV, Wasielewski MR, Hoffman BM. Science. 2010; 330:1075–1078. [PubMed: 21097931]
209. Yumoto T, Sagami I, Daff S, Shimizu T. J. Inorg. Biochem. 2000; 82:163–170. [PubMed: 11132623]
210. Haque MM, Fadlalla M, Wang ZQ, Ray SS, Panda K, Stuehr DJ. J. Biol. Chem. 2009; 284:19237–19247. [PubMed: 19473991]
211. Liu X-D, Mazumdar T, Xu Y, Getzoff ED, Eissa NT. J Immunol. 2009; 183:5977–5982. [PubMed: 19828635]
212. Galinato MGI, Spolitak T, Ballou DP, Lehnert N. Biochemistry. 2011; 50:1053–1069. [PubMed: 21158478]
213. Sevrioukova IF, Poulos TL. Arch. Biochem. Biophys. 2010; 507:66–74. [PubMed: 20816746]
214. Haque MM, Kenney C, Tejero J, Stuehr DJ. FEBS J. 2011 in press.
215. Jachymova M, Martasek P, Panda S, Roman LJ, Panda M, Shea TM, Ishimura Y, Kim JJP, Masters BSS. Proc Natl Acad Sci U S A. 2005; 102:15833–15838. [PubMed: 16249336]
216. Brunner K, Tortschanoff A, Hemmens B, Andrew PJ, Mayer B, Kungl AJ. Biochemistry. 1998; 37:17545–17553. [PubMed: 9860870]
217. Hay S, Brenner S, Khara B, Quinn AM, Rigby SEJ, Scrutton NS. J. Am. Chem. Soc. 2010; 132:9738–9745. [PubMed: 20572660]
218. Neese F, Solomon EI. Inorg. Chem. 1999; 38:1847–1865. [PubMed: 11670957]
219. Kirk ML, Peariso K. Curr. Opin. Chem. Biol. 2003; 7:220–227. [PubMed: 12714055]
220. Visser, SPd. Biochem. Soc. Trans. 2009; 037:373–377. [PubMed: 19290865]
221. de Visser SP, Tan LS. J. Am. Chem. Soc. 2008; 130:12961–12974. [PubMed: 18774806]
222. Menyhard DK. Chem. Phys. Lett. 2004; 392:439–443.
223. Floquet N, Hernandez J-Fo, Boucher J-L, Martinez J. J. Chem. Inf. Model. 2011; 51:1325–1335. [PubMed: 21574590]
224. Pushie MJ, George GN. The Journal of Physical Chemistry B. 2010; 114:3266–3275. [PubMed: 20158265]

225. Utesch T, Mroginski MA. The Journal of Physical Chemistry Letters. 2010; 1:2159–2164.

226. Feng CJ, Kedia RV, Hazzard JT, Hurley JK, Tollin G, Enemark JH. Biochemistry. 2002; 41:5816–5821. [PubMed: 11980485]

227. Feng C, Tollin G, Enemark JH. Biochim. Biophys. Acta. 2007; 1774:527–539. [PubMed: 17459792]

228. Johnson-Winters K, Tollin G, Enemark JH. Biochemistry. 2010; 49:7242–7254. [PubMed: 20666399]

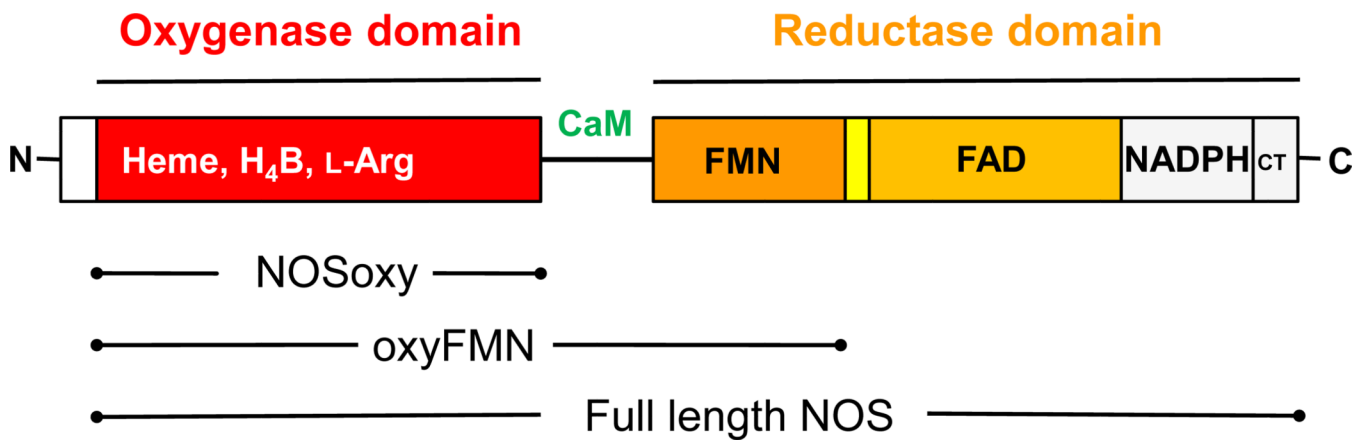

Figure 1.

Schematic illustration of the full-length NOS protein showing its oxygenase and reductase domains, and CaM-binding region that joins the two domains. The FMN domain, connecting domain (yellow), FAD/NADPH domain, and a C-terminal tail (CT) in the reductase domain are depicted. NOSred differs from P450 reductases primarily because of insertions and extensions related to control of NO synthesis. The NOS enzyme is a modular protein, and it is well accepted to study the catalytic mechanism by using the homologous truncated NOS constructs. Two typical truncated NOS constructs are shown: (i) NOSoxy and (ii) bi-domain oxyFMN construct (which is a minimal electron transfer complex designed to favor the interactions between the FMN and heme domains [36]).

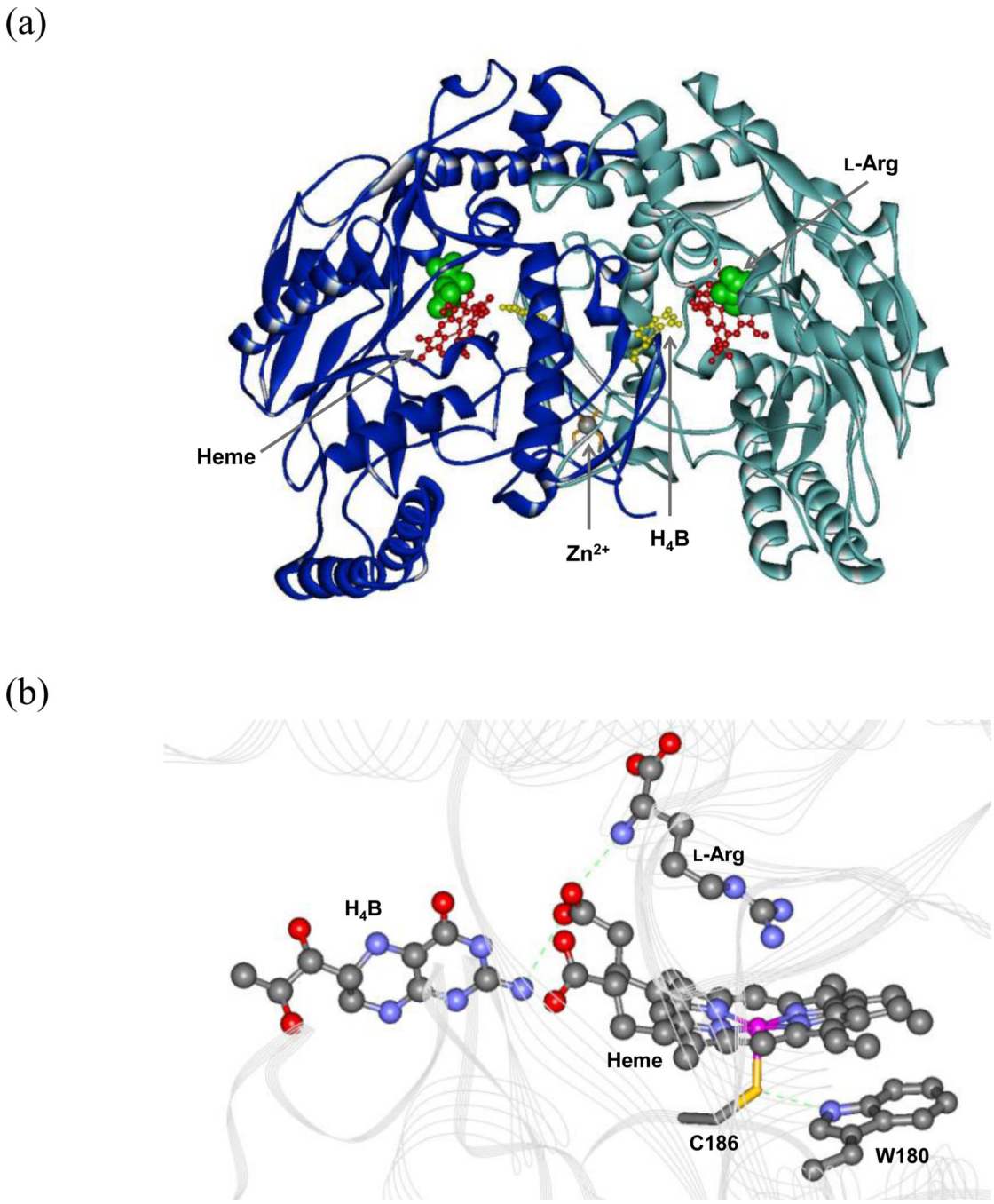

Figure 2.

(a) Dimeric structure of bovine eNOS heme domain showing L-Arg substrate (bound near the heme center), and H_4B and protoporphyrin IX cofactors. The two subunits are colored in dark blue and light blue, respectively. Each subunit contains the heme moiety, a substrate-binding site, a binding site for H_4B, which functions in electron transfer, and a tetra-coordinated zinc ion, which is important for structural integrity. Each subunit provides two of the cysteine ligands for zinc ion. (b) Structure of the ferric bovine eNOS active site showing *b*-type heme with coordinated Cys186, which hydrogen bonds to Trp180. Also note that the Trp180 side chain π-stacks with the heme. The L-Arg and H_4B are linked together

through a H-bonding network mediated by one of the two propionate groups of the heme. Generated from PDB file 2NSE.

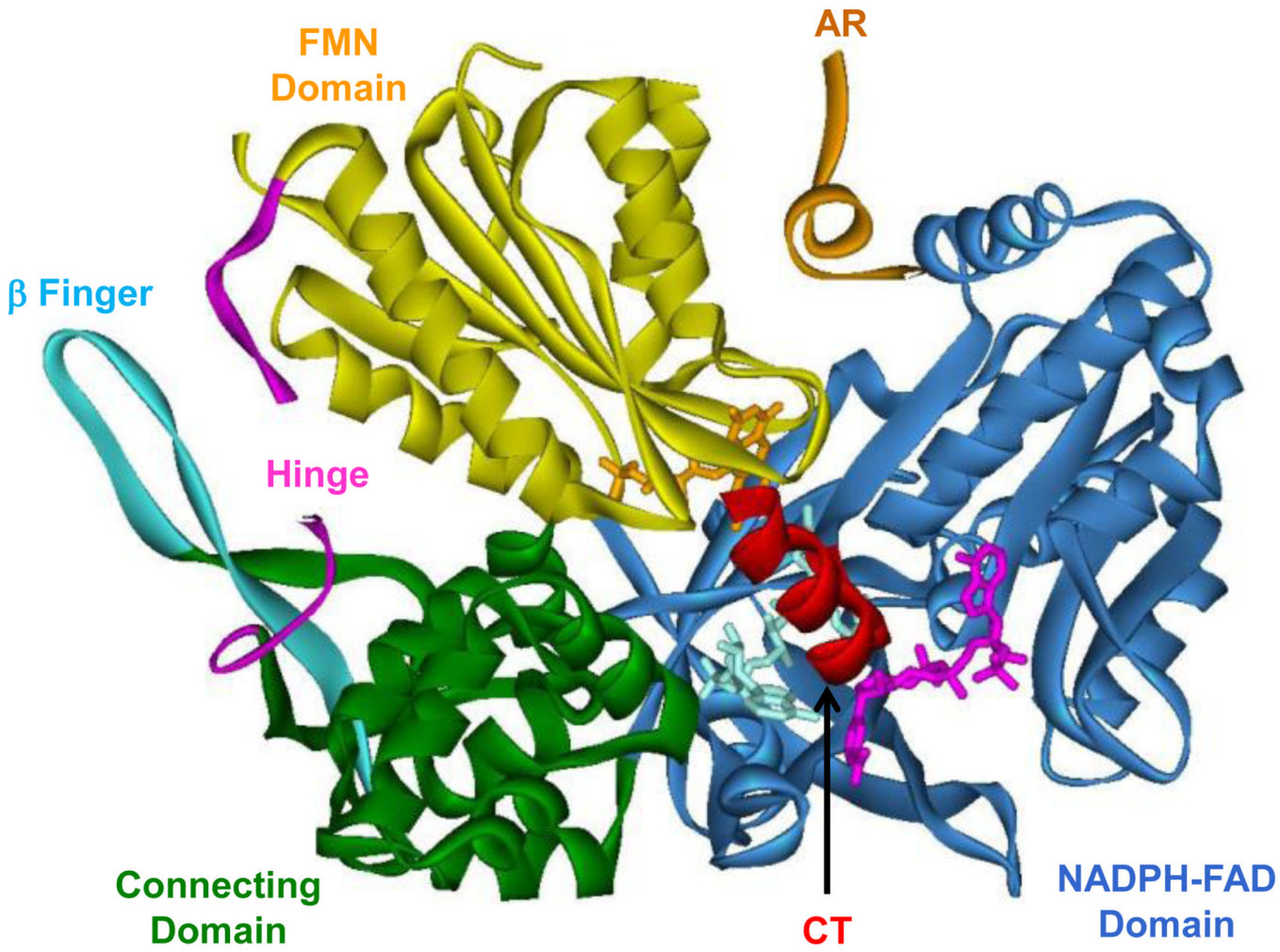

Figure 3.

Structure of an intact CaM-free rat nNOS reductase construct (PDB 1TLL); the ribbon diagram shows the FMN domain (yellow) docked against the NADPH/FAD domain (blue) in the FMN-shielded conformation. From the N to C terminus: FMN domain (yellow), connecting domain (green) with a flexible hinge (magenta) and a β-finger (cyan), NADPH-FAD domain (blue), and C-terminal tail (CT, red). $NADP^+$ (magenta) and cofactors FAD (light blue) and FMN (gold) are shown as stick representations. Because of their highly flexible nature, part of the AR insert within the FMN domain (gold) and hinge (magenta) regions were not well resolved in this structure.

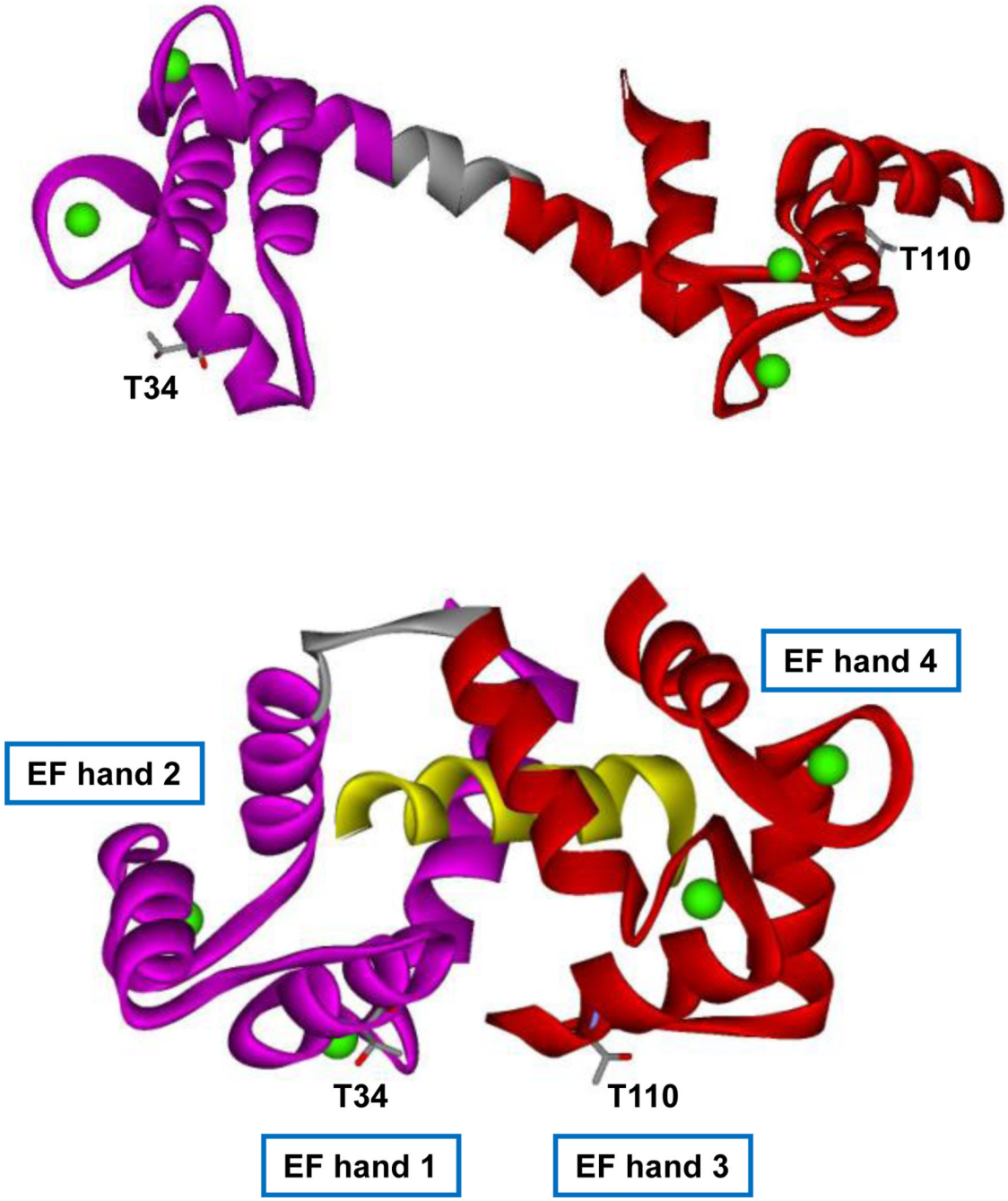

Figure 4.

Structures of Ca^{2+}/CaM alone (top) and bound to human eNOS CaM-binding region peptide (bottom); PDB 1CLL and 1NIW, respectively. Upon CaM binding to the eNOS-peptide, major conformational change occurs in the CaM structure, which forms a “latch” over the CaM-binding region. T34 and T110 are shown to demonstrate the dynamic conformational change CaM undergoes when bound to the eNOS peptide. The N- and C-terminal domains and central linker of CaM are shown in pink, red, and gray, respectively. Ca^{2+} ions are shown in green, and the eNOS peptide is shown in yellow.

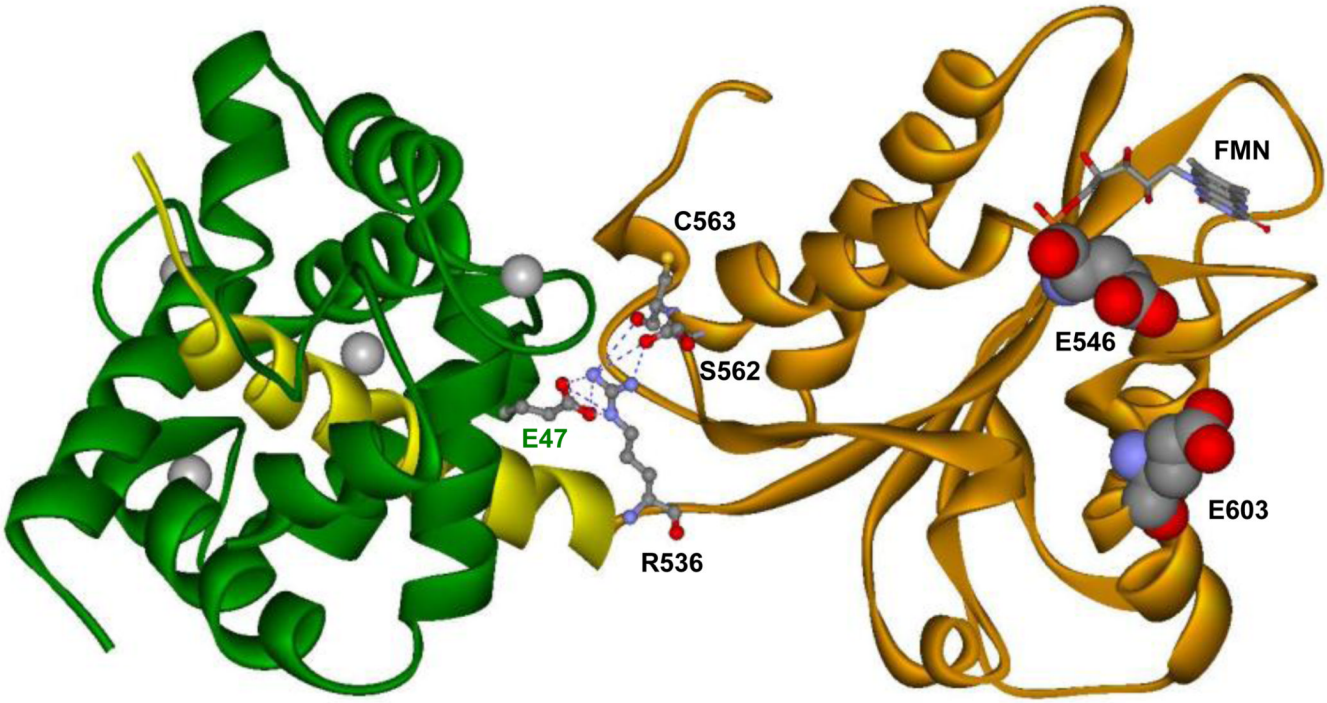

Figure 5.

Structure of a human iNOS FMN domain/CaM complex (PDB 3HR4). The FMN domain is gold, and the CaM-binding linker between the FMN and heme domains is yellow. The missing heme domain is at the other end of the CaM-binding linker. The CaM molecule is green, and Ca^{2+} ions are grey spheres. The bound CaM pivots on the R536(NOS)/E47(CaM) pair. R536 forms H-bonds with the backbone oxygens of S562 and C563 residues. Also note that E546 and E603 (shown in CPK) are charged surface residues located at the edge of the human iNOS FMN domain, and are conserved in the NOS isoforms.

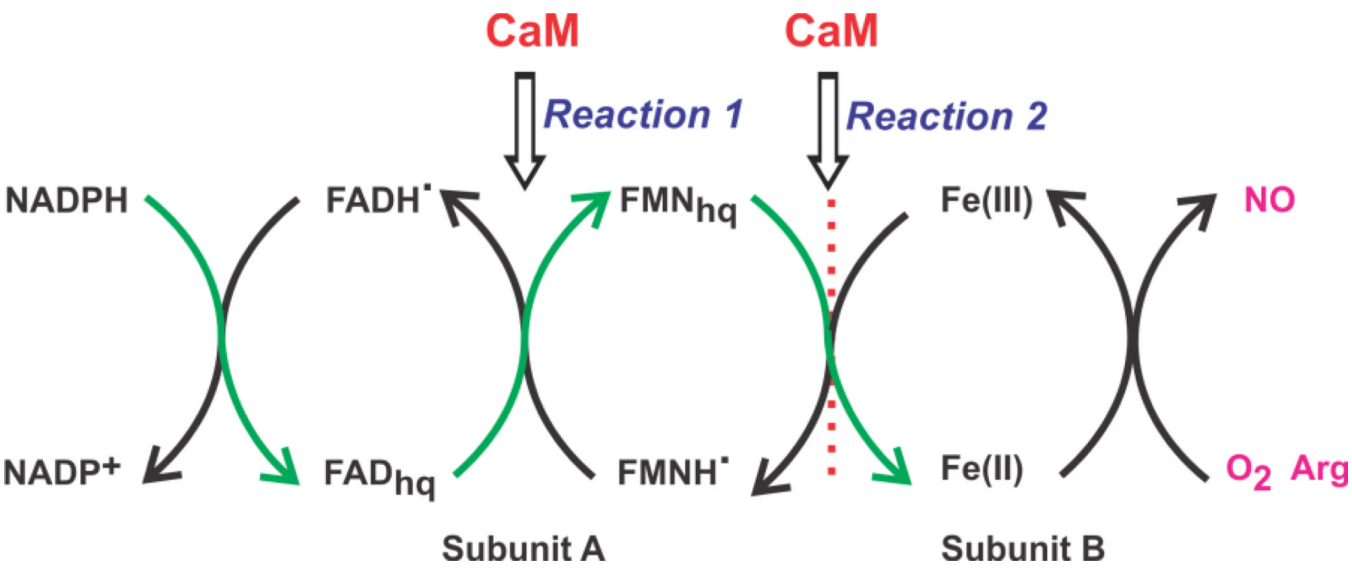

Figure 6.

Interdomain electron transfer (IET) processes (as shown in green arrows) in NOS from NADPH through FAD and FMN to heme (where binds and activates dioxygen). CaM binding activates the intersubunit FMN–heme IET (reaction 2) in eNOS and nNOS, and is also required for proper alignment of the FMN and heme domains in iNOS. The FMN–heme IET is essential for NOS function by delivery of electrons required for O_2 activation at the catalytic heme site. This IET step is also proposed to be important for reduction of the H_4B radical following hydroxylation of L-Arg substrate [145].

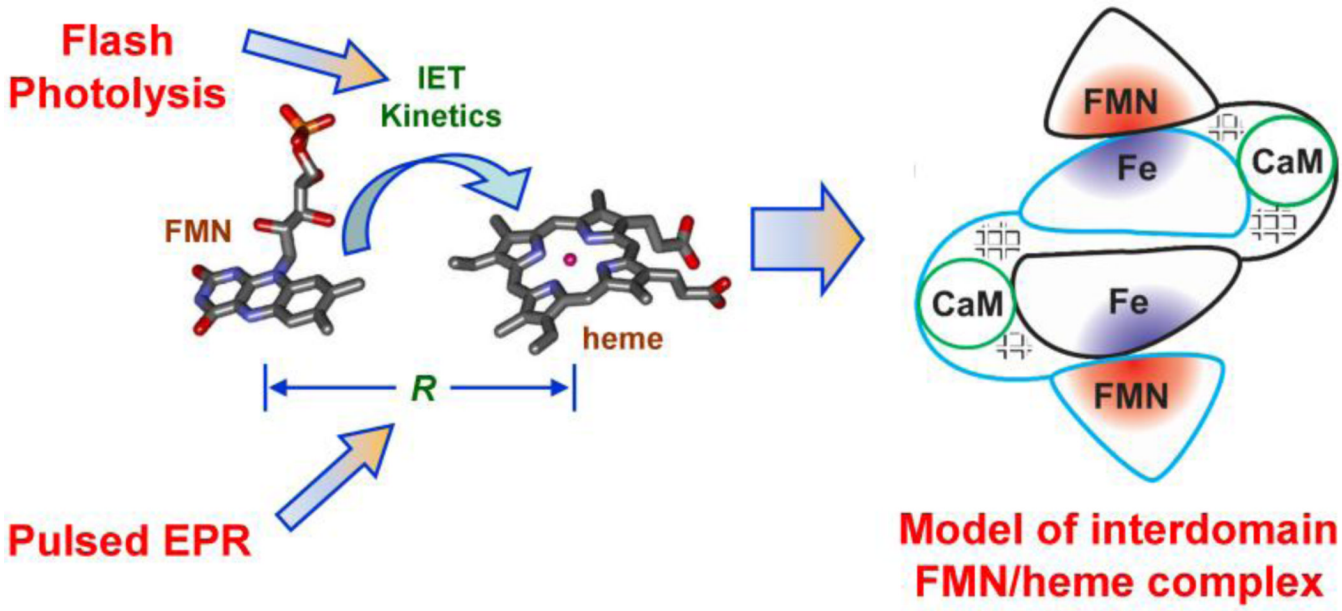

Figure 7.
Combined approach of laser flash photolysis (for determining the FMN–heme IET kinetics as a direct measure of the IET complex formation), pulsed EPR (for determining the FMN···Fe distance in the interdomain FMN/heme complex, and probing structure of heme active site), and site-directed mutagenesis (for modulating the key isoform-specific interactions).

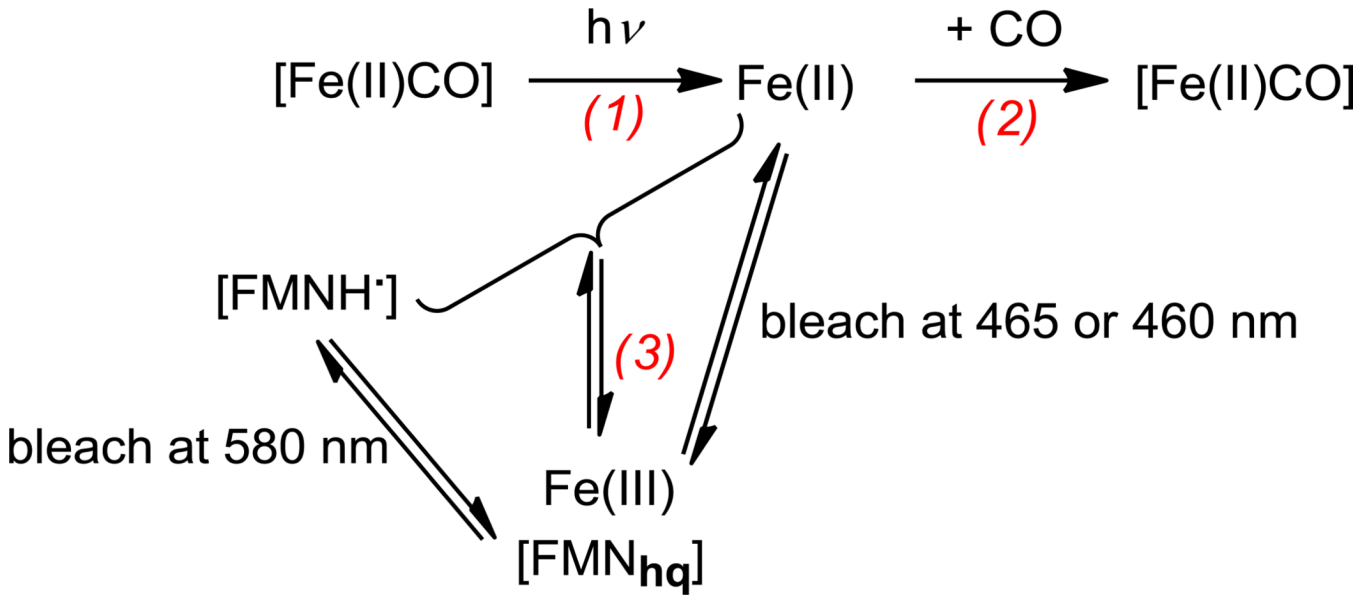

Figure 8.

Summary of processes occurring upon CO photolysis in the partially reduced form [Fe(II)-CO][FMNH•] of NOS proteins. A pulse of 450 nm laser is used to dissociate CO from the Fe(II)–CO complex with the formation of a transient free Fe(II) species (reaction 1). The laser-induced CO dissociation results in a drop of the midpoint potential of the heme, and rapidly converts a good electron acceptor (the Fe(II)–CO complex) into an electron donor (the free Fe(II) species), favoring electron transfer from Fe(II) to FMNH• (reaction 3). This IET process can be followed at 580 nm (that is due to FMNH• reduction), and 465 or 460 nm (for iNOS and nNOS respectively), which is due to heme oxidation. A CO/Ar (~ 1:3 v/v) mixture is used to slow down the CO rebinding (reaction 2), making it a poor competitor for the IET (reaction 3).

(a)

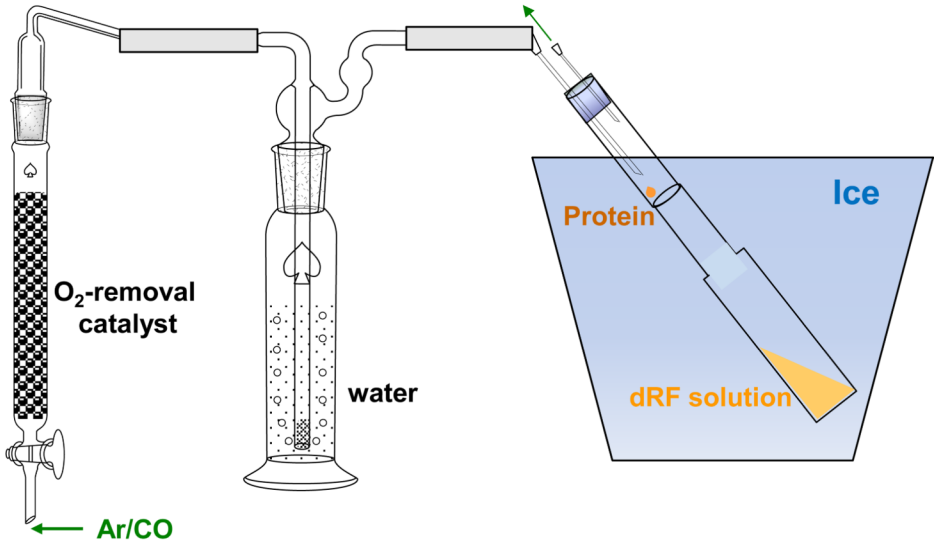

(b)

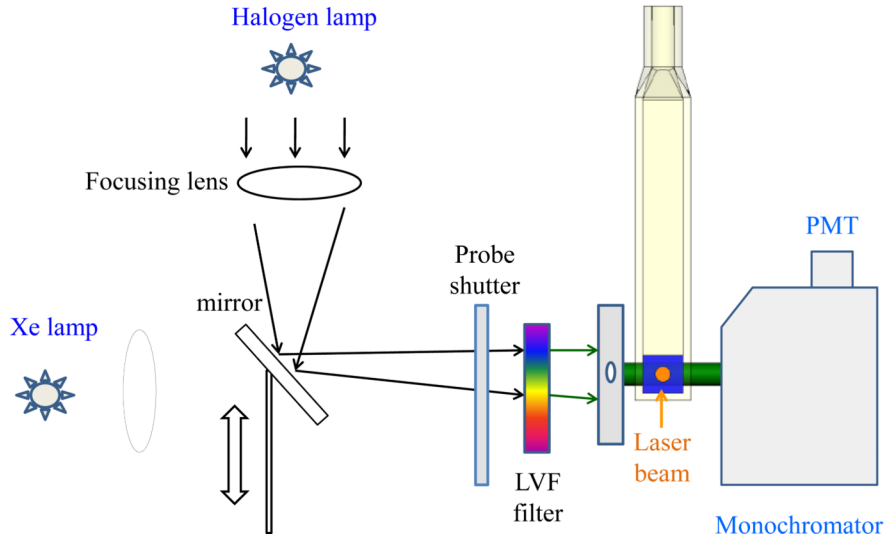

Figure 9.

(a) Schematic illustration of an Ar/CO gas manifold for degassing the sample. Argon and CO gases are pre-mixed (at a volume ratio of ~3:1), and pass through an oxygen-removing column and a bubbler before entering the laser flash photolysis cuvette. The cuvette joint section between the glass neck and quartz section provides a good place to leave the microliters protein aliquots for purging (before being mixed into the pre-degassed dRF solution in the buffer). The ice bath helps the removal of minor oxygen in the protein drops and stabilization of the protein. (b) Diagram of a customized laser flash photolysis system showing layout of the Xe arc and halogen lamps, liner variable filter (LVF, with adjustable band-pass), and alignment of the laser and monitor beams. The Xe and halogen lamps are

best used for measuring kinetics at ns-μs and ms-s time scales, respectively. Selection of the lamp can be realized by sliding the mirror back and forth.

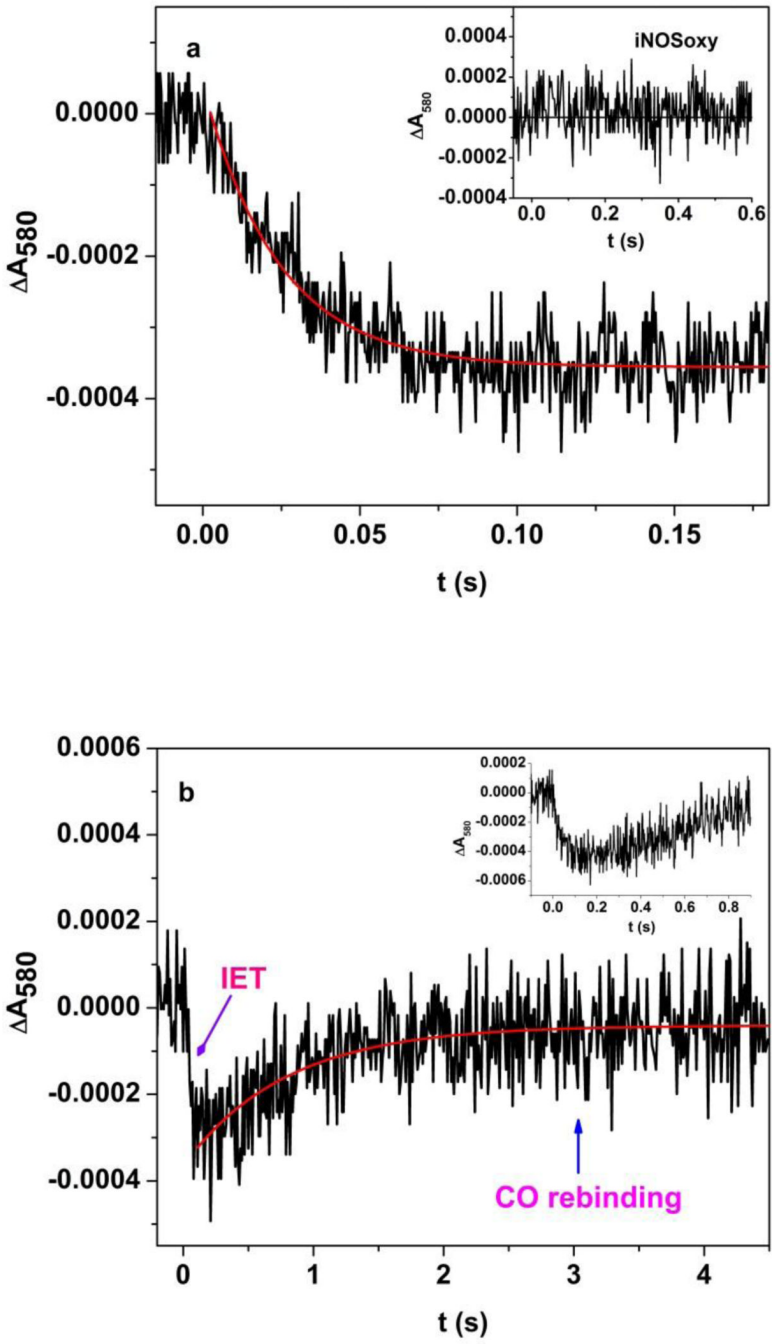

Figure 10.

Transient trace at 580 nm obtained at (a) ms and (b) seconds time scales of the [Fe(II)–CO] [FMNH•] form of a murine iNOS holoenzyme flashed by a pulse of laser. Note that FMNH• dominates the absorption in the range of 580–600 nm. As a control, the 580 nm absorption of the iNOSoxy construct (which does not contain FMN) stays above the baseline (inset of panel a). Note that rapid FMN–heme IET (as shown in panel a) occurs prior to the slower CO rebinding process; the transition is better depicted in inset of panel b. The solid line represents the best fit of the trace with a single-exponential decay model. Adapted from ref. [155].

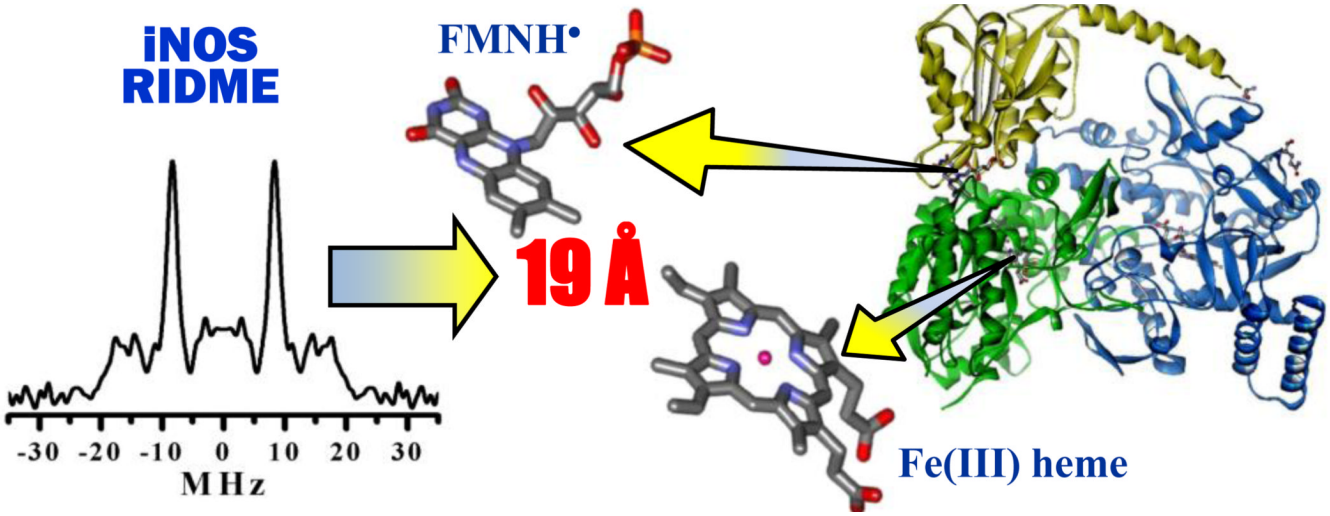

Figure 11.

The FMNH•–Fe(III) dipolar interaction spectrum obtained as a cosine FT of the ratio of time-domain RIDME traces recorded at 25 K and 15 K (to separate the dipolar ESEEM from that caused by magnetic nuclei). The FMN···Fe distance obtained (~ 19 Å) was used as a major constraint to select the computational docked FMN/heme complex (right side). The FMN and heme cofactors are shown in sticks. Note that the FMN domain (yellow) docks to oxygenase subunit A (green), and is covalently connected to the other oxygenase subunit B (blue), because the FMN–heme IET is inter-subunit [31]. The sample studied is of a human iNOS oxyFMN construct. Adapted from ref. [163].

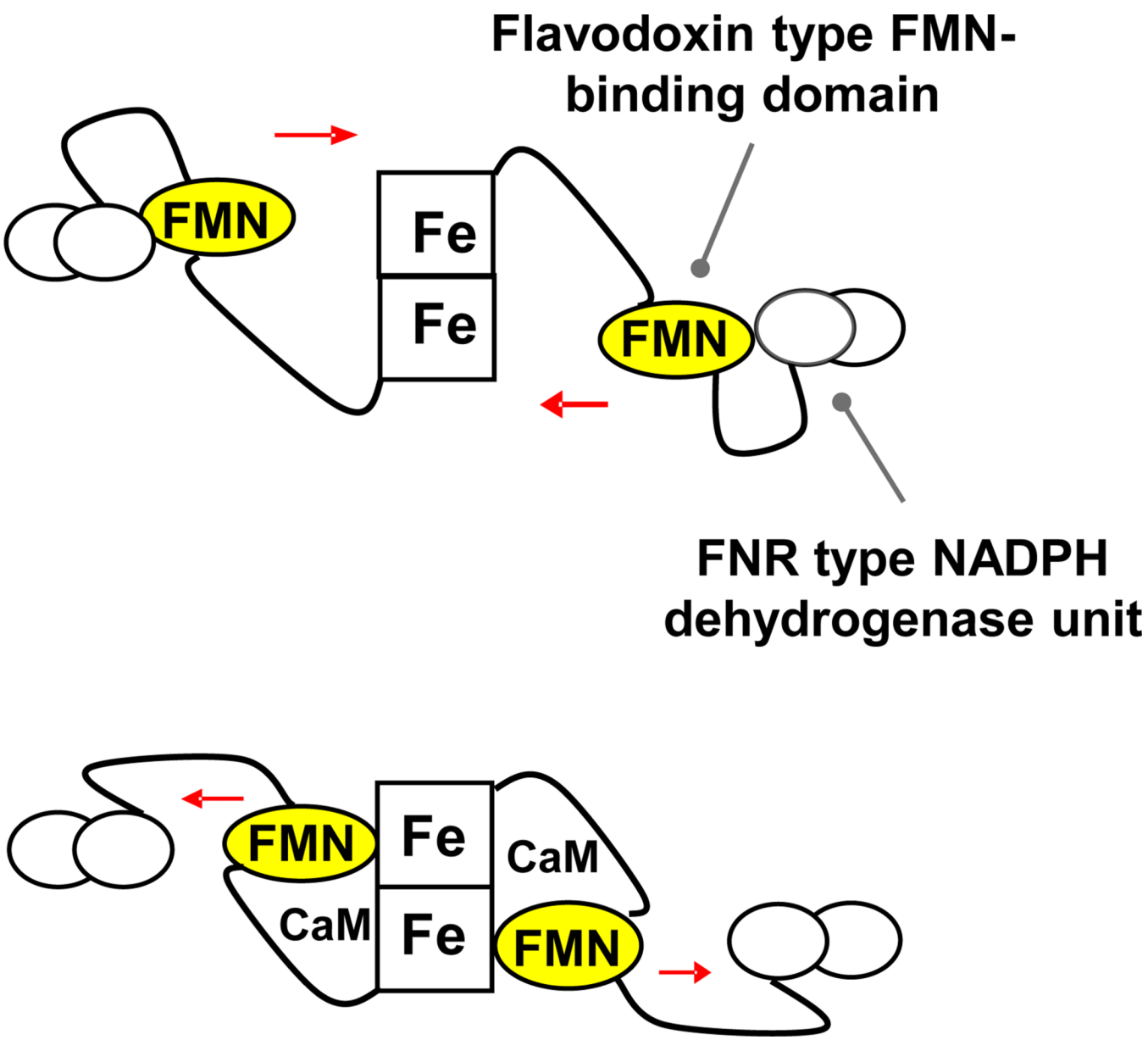

Figure 12.
Tethered shuttle model. Flavodoxin-type FMN-binding domain (yellow) shuttles between the flavodoxin-NADPH reductase (FNR)-type two-domain “dehydrogenase unit” and the heme-containing oxygenase domain. Top: input state; bottom: output state. The novel aspect of NOS is the involvement of CaM. CaM binding to eNOS/nNOS unlocks the input state, thereby enabling the FMN domain to shuttle between the FAD and heme domains. CaM is also required for proper alignment of the FMN and heme domains in iNOS. Adapted from ref. [157].

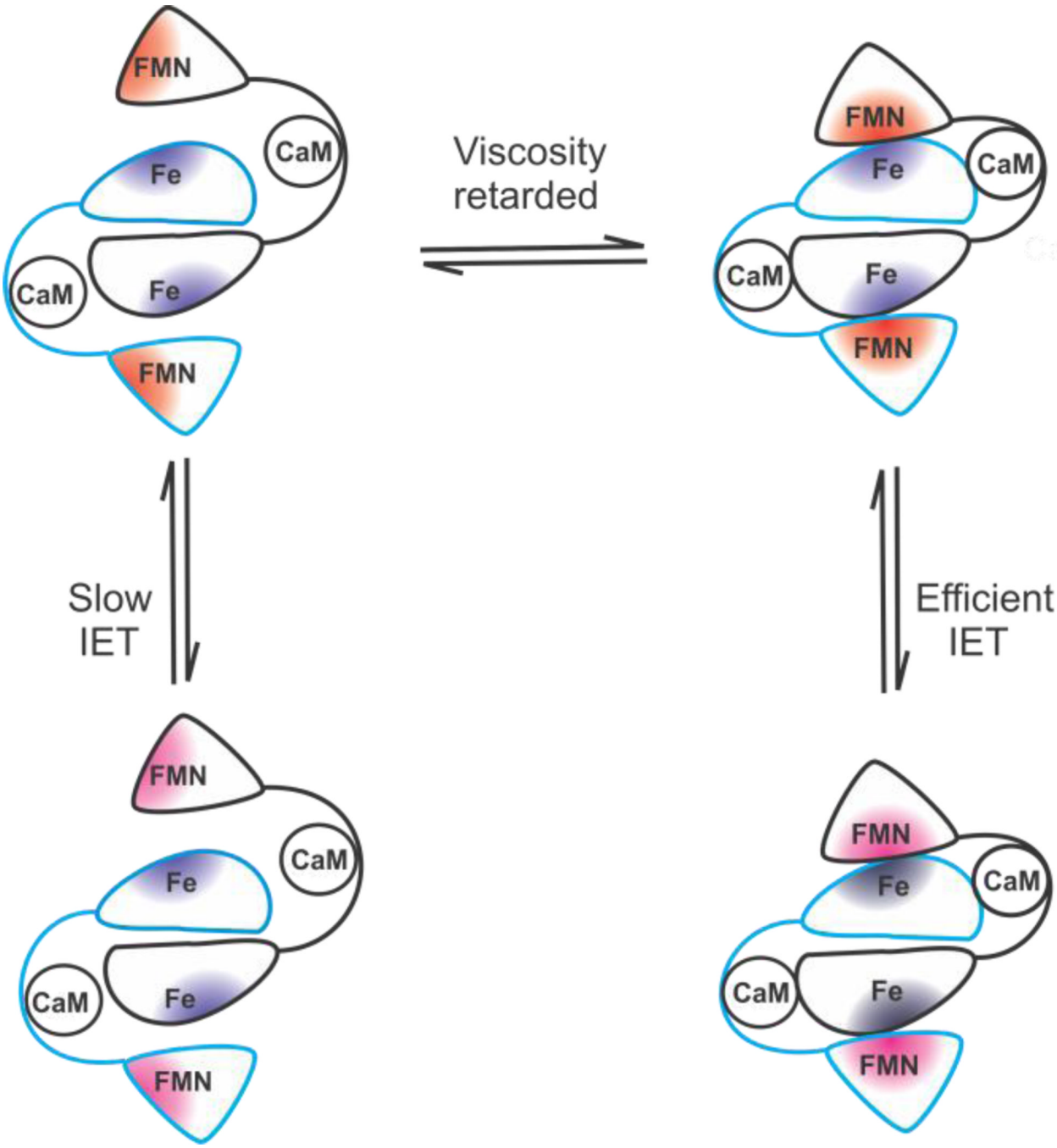

Figure 13.

Proposed mechanism of the CaM-controlled IET between the FMN and heme domains in NOS proteins. CaM binding to eNOS/nNOS allows a large conformational change of the FMN domain moving the FMN and Fe centers into close proximity, which results in efficient FMN–heme IET. The CaM-binding step is omitted because it is rapid [187]. The interdomain docking is guided by electrostatic interactions between the charged surface residues (red and blue regions) in the FMN and heme domains [199, 200]; also see Figure 14 below. The NOS FAD and NADPH binding domains are omitted for clarity.

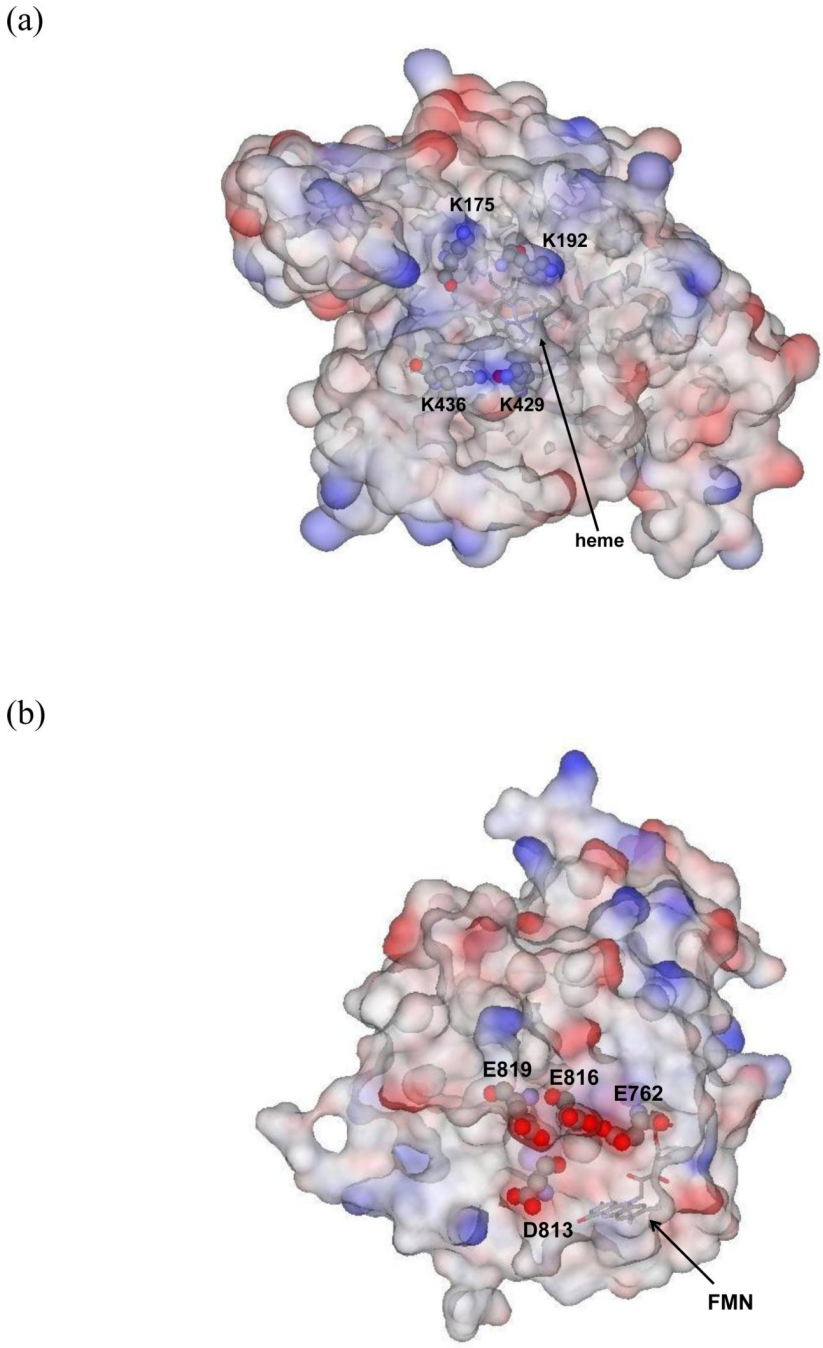

Figure 14.
Surface electrostatic potential distributions of (a) the human eNOS heme domain (PDB 3NOS), and (b) the FMN domain in the rat nNOS reductase construct (PDB 1TLL). Selected positively charged residues at the back face of heme and negatively charged residue at the edge of the FMN domain are labeled and shown in blue and red, respectively.

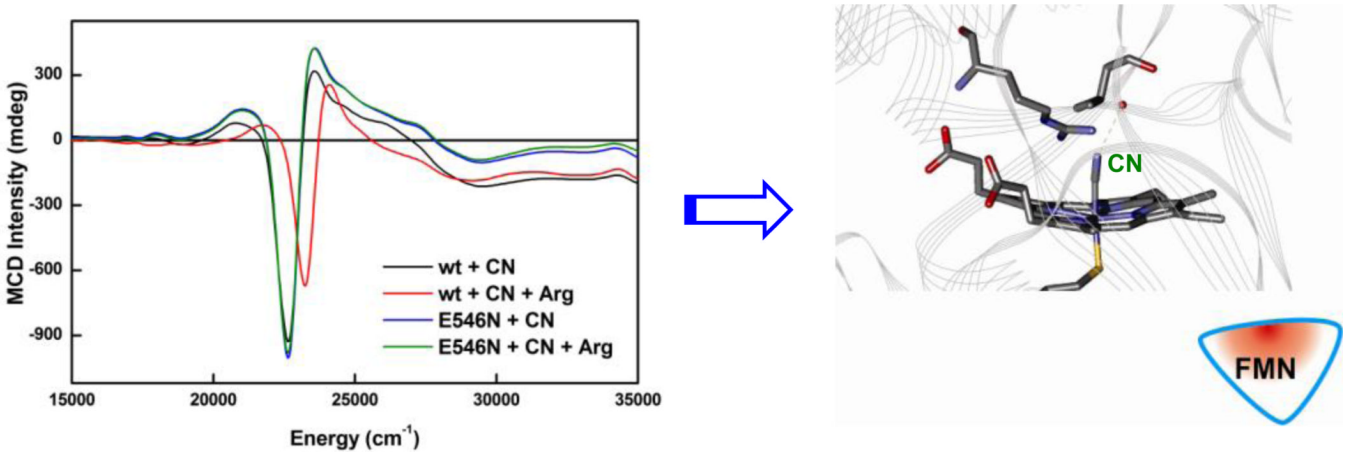

Figure 15.

MCD spectra (C-term) recorded at 5 K for ferric-cyano complexes in wild type (wt) and the E546N mutant of the human iNOS oxyFMN construct without or with L-Arg. Note that the MCD spectrum of the wt+CN^-+Arg sample (red trace) is significantly blue shifted (~ 600 cm^{-1}) relative to the other spectra. These results indicate that the docked FMN domain affects the key interaction between the L-Arg substrate and the axial ligand (*i.e.* CN^-) of the catalytic heme center located in an adjacent domain in iNOS. Adapted from ref. [170].

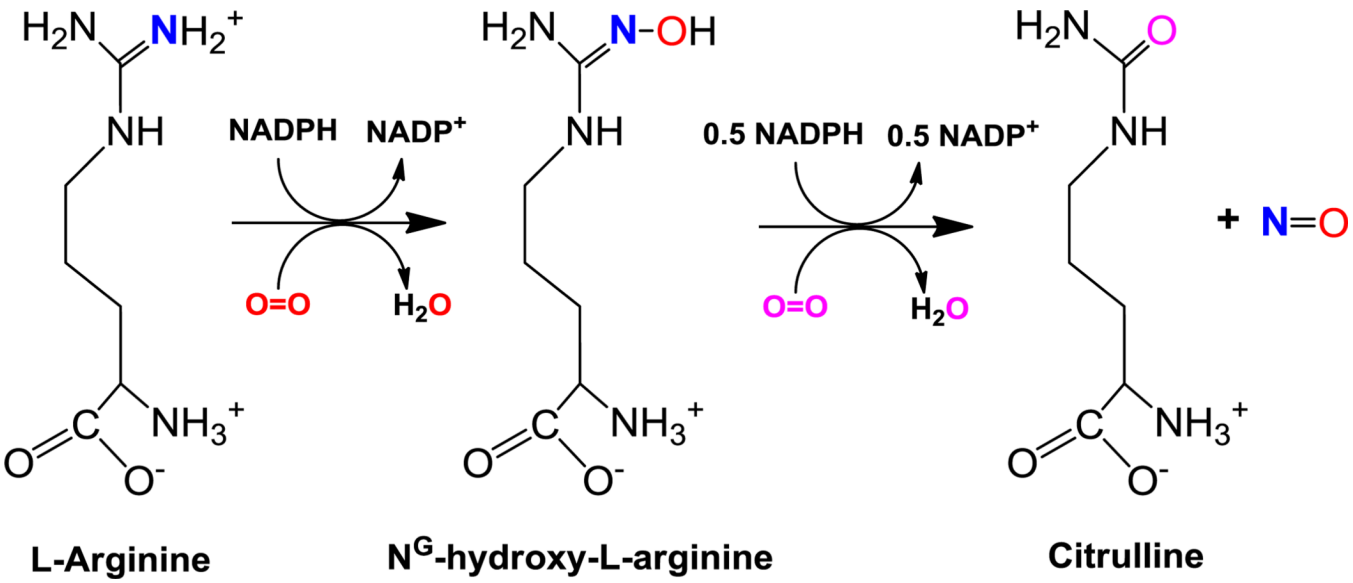

Scheme 1.
Production of NO by NOS enzyme.

Table 1

Combined spectroscopic, rapid kinetics and mutagenesis approach in studying the NOS IET and interdomain interactions.

Technique		Results	Information obtained from the data
Pulsed EPR	RIDME/ELDOR	FMN···Fe distance, distance distribution and relative orientation of the paramagnetic FMN and heme centers in NOS	Structural information of the interdomain complex and a key constraint of the computational IET complexes
	ENDOR/ESEEM	1^{st} and 2^{nd} sphere coordination environment of the heme site (type of magnetic nuclei, distance and direction)	Detailed insight into the heme active site structure, particularly of the axial ligand
Combined VTVH MCD/CW EPR		Ground spin state and spin-Hamiltonian parameters of the heme center (i.e. *g*, *D*, *E*)	Quantitative determination of heme electronic structure
Laser flash photolysis		Kinetics of the FMN–heme IET process	A measure of the IET complex formation
Site-directed mutagenesis		Mutation-dependent changes in the spectroscopic and IET kinetics properties	Roles of specific residues in regulating NOS function by the key interdomain interactions